Journal of the North for Basic and Applied Sciences, Vol. (8), Issue (2), (November 2023/ Rabi' II 1445 H) 89-124

KINGDOM OF SAUDI ARABIA
Northern Border University (NBU)
Journal of the North for Basic & Applied Sciences(JNBAS)
p - ISSN : 1658 -7022 / e-ISSN: 1658 - 7014
www.nbu.edu.sa
s.journal@nbu.edu.sa

Optimal Power Flow Considering Solar and Wind Energy Systems Via Modified Cuckoo Optimization Algorithm

Abdulaziz Alanazi *

(Received 2/4/2023 ; accepted 6/9/2023)

Abstract: By considering a variety of objective functions, this paper has created an evolutionary method that is both effective and reliable for resolving the problem of multi-constraint optimal power flow (OPF). It proposes a multiobjective OPF model that considers renewable energy sources in numerous scenarios. This model optimizes fuel costs, emissions, power losses, and voltage fluctuations. The modified Cuckoo optimization algorithm (MCOA) is also suggested for finding optimized and satisfactory load flow solutions. The model is tested against eight scenarios over IEEE 30-bus and IEEE 118-bus networks, considering multiple objective functions. Optimal results demonstrate the effectiveness of MCOA for multiobjective OPF with various constraints compared to other algorithms studied in recent literature.

Keywords: Multi-constraint OPF, Local search, Cuckoo Optimization Algorithm, MCOA, Solar and wind energy units, Non-smooth cost functions

DOI: 10.12816/0061647

* **Corresponding Author:**
Assistant Professor, Electrical Engineering Dept., College of Engineering, Northern Border University, P.O. Box: 1321, Code: 91431, Arar, Kingdom of Saudi Arabia.

e-mail: af.alanazi@nbu.edu.sa

المملكة العربية السعودية
جامعة الحدود الشمالية (NBU)
مجلة الشمال للعلوم الأساسية والتطبيقية (JNBAS)
طباعة ردمد: 1658-7022/ إلكتروني – ردمد: 1658-7014
www.nbu.edu.sa
http://jnbas.nbu.edu.sa

التدفق الأمثل للطاقة مع مراعاة أنظمة الطاقة الشمسية وطاقة الرياح من خلال خوارزمية تحسين الوقواق المعدلة

عبدالعزيز فريح العنزي*

(قدم للنشر في 1444/9/11هـ؛ وقبل للنشر في 1445/2/21هـ)

مستخلص البحث: من خلال النظر في مجموعة متنوعة من الوظائف الموضوعية، أنشأت هذه المقالة طريقة تطورية فعالة وموثوقة لحل مشكلة تدفق الطاقة الأمثل متعدد القيود (OPF). حيث تقترح نموذج OPF متعدد الأهداف الذي يأخذ في الاعتبار مصادر الطاقة المتجددة في سيناريوهات عديدة. يعمل هذا النموذج على تحسين تكاليف الوقود والانبعاثات وفقدان الطاقة وتقلبات الجهد. تم أيضًا اقتراح خوارزمية تحسين الوقواق (MCOA) المعدلة للعثور على حلول تدفق الحمل الأمثل والمرضية. تم اختبار النموذج مقابل ثمانية سيناريوهات عبر شبكات IEEE 30-bus وIEEE 118-bus، مع الأخذ في الاعتبار وظائف موضوعية متعددة. توضح النتائج المثالية فعالية MCOA لـ OPF متعدد الأهداف مع قيود مختلفة مقارنة بالخوارزميات الأخرى التي تمت دراستها في الدراسات الحديثة.

كلمات مفتاحية: التدفق الأمثل للطاقة متعدد القيود، البحث المحلي، خوارزمية تحسين الوقواق، خوارزمية تحسين الوقواق المعدلة، وحدات الطاقة الشمسية وطاقة الرياح، وظائف التكلفة غير السلسة

*** للمراسلة:**
أستاذ مساعد، قسم الهندسة الكهربائية، كلية الهندسة، جامعة الحدود الشمالية ص ب: 1321 رمز بريدي: 91431 ، عرعر، المملكة العربية السعودية.

e-mail: af.alanazi@nbu.edu.sa

DOI: 10.12816/0061647

1. Introduction

In today's engineering world, there is no standard and comprehensive way to address the problematic optimization issues of many sectors. Hence, hundreds of alternative strategies have been created recently, frequently proving their efficacy in handling specific optimization issues. One of the complicated challenges in engineering is optimal power flow (OPF), which is of significant significance in designing power systems (Ghasemi, Ghavidel, Gitizadeh, et al., 2015). The basic topic of OPF has been garnering the attention of researchers in the area of electrical engineering for more than 50 years. The first simplified issue is the OPF problem for vast networks (Ghasemi, Ghavidel, Gitizadeh, et al., 2015). In the past, researchers employed solution strategies based on mathematical methods such as nonlinear programming (NLP) (Alsac & Stott, 1974) to address these difficulties. Heuristic solutions were employed to address the OPF issue in the following. The difficulty of the actual OPF issue (owing to its nonlinear, non-convex and non-derivative character) has motivated academics to develop novel optimization approaches to address the problem in recent years.

Researchers have suggested the teaching-learning-based improvement (TLBO) algorithmic program increased with Lévy mutation (LTLBO) (Ghasemi, Ghavidel, Gitizadeh, et al., 2015), a modified lepidopteron swarm algorithm (MMSA) (Elattar, 2019) to account for indirect, overstated, and underestimated expenses connected with renewable energy systems. This endeavour aims to reduce the financial strain placed on businesses. Multiobjective accommodative guided differential evolution (DE) (Duman et al., 2021), a more effective method for multiobjective optimization of manta hunting (IMOMRFO) is presented in (Kahraman et al., 2022). Multiobjective mayfly algorithm (MOMA) (Kyomugisha et al., 2022), a particle swarm optimization (PSO) (Hazra & Sinha, 2011), Jaya algorithm (Warid et al., 2016), chaotic invasive weed optimization algorithms (CIWO) (Ghasemi, Ghavidel, Akbari, et al., 2014), and an algorithm for identifying new bacteria (MBFA) (Panda et al., 2017). At the level (Shi et al., 2011), a newly developed hybrid algorithmic program for the protection of OPF required the utilization of wind and heat generators. An new improved adaptive DE (Li et al., 2020), adaptive cluster search optimization (AGSO) (Daryani et al., 2016), ant lion algorithm (Maheshwari et al., 2021), the multiobjective First State algorithmic program (Elattar & ElSayed, 2019), the enhanced colliding bodies improvement (ICBO) (Bouchekara et al., 2016), BAT search algorithmic program (Venkateswara Rao & Nagesh Kumar, 2015), and the salp swarm algorithmic program (SSA) (Kamel et al., 2021). Improved artificial bee colonies (IABCs) (Khorsandi et al., 2013), multiobjective dynamic OPFs (Ma et al., 2019), the Harris hawks improvement (HHO) technique (Islam et al., 2020), a hybrid of phasor PSO (PPSO), and attraction search (PPSO-GSA) (Ullah et al., 2019) are also examples of recent developments in this field.

A novel hybrid firefly-bat algorithmic program with a constraints-priority object-fuzzy sorting approach has been developed and named gray wolf improvement (GWO) (Khan et al., 2020). This program is based on the firefly, and the bat (HFBA-COFS) (Chen et al., 2019), a hybrid PSO-GWO (Riaz et al., 2021) algorithmic program is created by combining the particle swarm optimization (PSO) method with the gray wolf optimization (GWO) algorithm. An anticipated security value dynamic OPF (ESCDOPF) with a hybrid system that makes use of both star resources and flexible resources (Kumari & Vaisakh, 2022), a bird swarm algorithmic program (BSA) (Ahmad et al., 2021), a chaotic Pan troglodytes optimizer (CBO) (Hassan et al., n.d.). Tunicate swarm algorithm (TSA) (El-Sehiemy, 2022), a modified flow of a water-based optimizer (TFWO) (Sarhan et al., 2022), and an improved hybrid PSO and GSA (PSOGSA) integrated with chaotic maps (CPSOGSA) for OPF with random alternative energy and FACTS devices (Duman, Li, et al., 2020). A new cross entropy-cuckoo search algorithm (CE-CSA) (Sarda et al., 2021), and a hybrid PSO and shuffle frog leap algorithmic program (SFLA) (Narimani et al., 2013).

Program with an improved algorithm for maximizing Pareto efficiency outlined in (Yuan et al., 2017) is three significant enhancements that have been made to the preliminary version of the algorithmic software for the Pareto organic process. To get things started, the population size of the external archive is just the number of persons who have a subordinate position in the choice operator of the surrounding environment. Second, the population of the external archive is maintained up to date by using the geometer distance between the elite and their *k*-th closest neighbours. This keeps the population of the external archive accurate. Thirdly, the native search approach is included in the algorithmic program that makes up the strong Pareto organic process. The two-point estimation methodology (TPEM) (Saha et al., 2019), the social spider improvement algorithms (SSO) (Nguyen, 2019), and sine-cosine algorithm (SCA) (Attia et al., 2018; Dasgupta et al., 2020). The cuckoo optimization algorithm (COA) (Rajabioun, 2011) is a powerful and frequently used evolutionary optimization technique. It was invented by Ramin Rajabion in 2011 and is named after its namesake. This idea, which was first inspired by the cuckoo's habit of laying eggs and subsequently evolved to encompass the practice of stealing eggs from one's neighbours, has found application in a variety of industries like increasing lagrangian relaxation unit commitment (Zeynal et al., 2014), optimum coordination of directed overcurrent relays in microgrids (Dehghanpour et al., 2016), and electrical power system forecasting (Xiao et al., 2017), extreme learning machine for categorization of medical data (Mohapatra et al., 2015), etc.

It has been shown, however, that when used in complicated nonlinear circumstances, the technique risks being trapped in a local solution and losing the ability to optimize the solution (Dalali & Kazemi Karegar, 2016). The literature review shows that an efficient version of the COA has yet to be proposed for optimizing the various kinds of OPF problems. Also, some other optimization algorithms reviewed require improvements in robustness, finding better solutions, avoiding local optimal solutions, and improving convergence properties. Thus, this paper employs a new migration operator to balance the exploration-exploitation process strategically and improve the quality of optimal solutions through COA. The analysis of eight cases with different objectives on the IEEE 30-bus and IEEE 118-bus networks illustrated the cost-emission-effective scheduling of thermal power plants using renewable energies. Moreover, the simulation results demonstrate the MCOA's effectiveness and validity compared with other recently published algorithms for solving OPF problems. This study employs one of the effective strategies that has been applied in the past to maximize various load dispatch challenges in the two solar-and-wind-powered combined power systems.

Here are the main contributions of this paper:

1) Introducing a novel, efficient, and robust version of conventional cuckoo optimization algorithms, namely modified cuckoo optimization algorithms (MCOA), for optimizing optimal power flow (OPF) problems involving conventional thermal power plants and renewable energy sources, including solar photovoltaics and wind power distributed generation systems.
2) To address the uncertainties of renewable generations, in this work, the Weibull probability density function models the wind distribution, whereas the lognormal probability density function models the solar irradiation.
3) As part of the OPF problem, fuel costs, emissions, power losses, and voltage deviations are considered. These functions are constrained by economic, technical, and safety factors. Aside from the production cost of thermal power units, this study also considered reserve, direct, and penalty costs.
4) The amount of carbon tax is linked to the goal function to examine the potential effects of renewable energies on the optimal scheduling of thermal power plants in a cost-emission-effective manner.
5) Comparing the proposed MCOA and other recently published algorithms on the IEEE 30-bus and IEEE 118-bus networks to illustrate their effectiveness and validity.

This research continues in the following four sections: section 2, in which we discuss the formulation of OPF issues; section 3, in which we explain the concepts and structure of COA; and sections 4 and 5, in which we offer the proposed MCOA algorithm to solve OPF in the IEEE 30-bus and IEEE 118-bus networks, respectively. We will display and debate the simulation's results in the fourth part. In the concluding part, labelled "Conclusions," 6 will summarize the study's findings.

2 . OPF Problem Formulation

Solving the OPF problem involves determining and controlling a set of control variables to optimize the objectives in the operation of an electric network (while balancing all practical constraints). A primary goal is to minimize production costs while satisfying electrical demands.

A multiobjective OPF with different constraints is presented in this study as an alternative to other algorithms studied in the recent literature. The following expression is used to create a typical OPF problem (Ghasemi, Ghavidel, Gitizadeh, et al., 2015):

$$MinF(u,x) \quad (1)$$

$$h(u,x) \leq 0 \quad (2)$$

$$g(u,x) = 0 \quad (3)$$

Within these associations, u and x represent, respectively, the independent and the control variables.

In addition, the objective function consists of a collection of equality requirements and a set of inequality constraints that pertain to the issue.

2.1 Control variables

The following are examples of control variables that are involved in OPF issue relationships (Ghasemi, Ghavidel, Gitizadeh, et al., 2015):

1. $P_{G_2}, \ldots, P_{G_{NG}}$ The active power generated in the PV bus, except for the slack bus
2. $V_{G_1}, \ldots, V_{G_{NG}}$ Voltage range in PV buses
3. $Q_{C_1}, \ldots, Q_{C_{NC}}$ Compensation of parallel reactive amperes
4. $T_1, \ldots, T_{NT}$ Adjustment of tap transformers

According to the control variables, u is included:

$$u^T = \left[Q_{C_1}, \ldots, Q_{C_{NC}}, V_{G_1}, \ldots, V_{G_{NG}}, P_{G_2}, \ldots, P_{G_{NG}}, T_1, \ldots, T_{NT}\right] \quad (4)$$

Where *NG*, *NC* and *NT* show the number of generators, reactive power compensators and tap-changer transformers.

2.2 State variables

The set of state variables in OPF problem relationships include the following (Ghasemi, Ghavidel, Gitizadeh, et al., 2015):

1. P_{G_1} :Active production power in slack bass
2. $V_{L_1}, \ldots, V_{L_{NPQ}}$ Voltage range in load buses
3. $Q_{G_1}, \ldots, Q_{G_{NG}}$ Output reactive power of production units
4. $S_{l_1}, \ldots, S_{l_{NTL}}$ Power loading in the lines

So, x is included:

$$x^T = \left[S_{l_1}, \ldots, S_{l_{NTL}}, Q_{G_1}, \ldots, Q_{G_{NG}}, V_{L_1}, \ldots, V_{L_{NPQ}}, P_{G_1}\right] \quad (5)$$

where the numbers represent the bus bars, network lines, and total lines (*NPQ*, *NTL*, and *NG*).

2.3 Equality constraints

The problem's insistence on equality places restrictions on how we may approach it, as discussed in this section. The technical status of the power network, as defined by OPF relations, is described by the parity constraints, also known as physical constraints, in OPF. This may convey these restrictions through the majority of the following links (Ghasemi, Ghavidel, Gitizadeh, et al., 2015):

$$P_{Gi} - P_{Di} - V_i \sum_{j=1}^{NB} V_j\left[B_{ij} \sin\ (\delta_i - \delta_j) + G_{ij} \cos\ (\delta_i - \delta_j)\right] = 0 \quad (6)$$

$$Q_{Gi} - Q_{Di} - V_i \sum_{j=1}^{NB} V_j\left[G_{ij} \sin(\delta_i - \delta_j) - B_{ij}\, cos(\delta_i - \delta_j)\right] = 0 \quad (7)$$

Let's break this issue down into its component components to make things clearer:

"i" and "j" are bus number indices; "*Vi*" and "*Vj*" are voltage magnitudes; "*PGi*" and "*QGi*" are real and reactive power outputs from the generator; and "*QDi*" and "*PDi*" are real and reactive power demands from the load. Let's begin with "i" and "j" as these are the array indices. The following table details the susceptance *Bij* and conductance *Gij* of the branch connecting bus i and bus j, as well as the phase angle $(\delta_i - \delta_j)$ between the voltages of the buses and the total number of buses in the system.

2.4 Inequality constraints

The following are some technical limitations put on generators for i=1, 2, …, *NG* (Ghasemi, Ghavidel, Gitizadeh, et al., 2015):

$$V_{Gi}^{min} \leq V_{Gi} \leq V_{Gi}^{max} \quad (8)$$

$$P_{Gi}^{min} \leq P_{Gi} \leq P_{Gi}^{max} \quad (9)$$

$$Q_{Gi}^{min} \leq Q_{Gi} \leq Q_{Gi}^{max} \quad (10)$$

In this equation, V_{Gi}^{min} and V_{Gi}^{max} represent the minimum and maximum magnitudes of voltage for the ith unit, $P_{Gi}^{min}$and P_{Gi}^{max}represent the minimum and maximum values of real power for the ith unit, and $Q_{Gi}^{max}$and Q_{Gi}^{min}represent the maximum and minimum allowable values of reactive generation for the ith generator.

Furthermore, the following connections illuminate the technical limitations of transformers and parallel VAR compensators:

$$T_i^{min} \leq T_i \leq T_i^{max} \quad (11)$$

$$Q_{Ci}^{min} \leq Q_{Ci} \leq Q_{Ci}^{max} \quad (12)$$

where $T_i^{max}$and $T_i^{min}$are the maximum and lowest taps of transformers for $i = 1, \ldots, NT$ that may be used to change the tap of the ith transformer. The range of VAR of the compensating compensators for $i = 1, \ldots, NC$ is denoted by $Q_{Ci}^{min}$and Q_{Ci}^{max}.

Finally, the following are some of the limitations of network security:

- The bus bar voltage constraints

As stated in (13), the voltage of system bus bars must be selected between the upper V_{Li}^{min} and lower V_{Li}^{max} limitations.

$$V_{Li}^{min} \leq V_{Li} \leq V_{Li}^{max}; i = 1, 2, \ldots, NPQ \quad (13)$$

- Power in transmission lines

The power in the network lines for $i = 1,2, \ldots, NTL$ should fulfill the relation (14):

$$S_{li} \leq S_{li}^{max} \quad (14)$$

S_{li} and S_{li}^{max} signify the apparent power through ith transmission line and its higher range.

2.5 Control constraints

In order to consider the violation of the constraints of a penalty function, it is considered as follows (Ghasemi, Ghavidel, Gitizadeh, et al., 2015):

$$J = \sum_{i=1}^{NG} F_i(P_{Gi}) + \lambda_S \sum_{i=1}^{NTL} (S_{li} - S_{li}^{\lim})^2 + \lambda_V \sum_{i=1}^{NPQ} (V_{Li} - V_{Li}^{\lim})^2 + \lambda_Q \sum_{i=1}^{NG} (Q_{Gi} - Q_{Gi}^{\lim})^2 + \lambda_P (P_{G1} - P_{G1}^{\lim})^2 \quad (15)$$

where x^{lim} is a variable that is specified in the following equation as an auxiliary variable, where λ_S, λ_V, λ_Q, and λ_P are the punishment factors (Ghasemi, Ghavidel, Gitizadeh, et al., 2015):

$$x^{\lim} = \begin{cases} x & x^{\min} \leq x \leq x^{\max} \\ x^{\max}; & x > x^{\max} \\ x^{\min}; & x < x^{\min} \end{cases} \quad (16)$$

3 The Proposed Optimizer

3.1 COA overview

The key phases of the cuckoo bird optimization technique may be broken down (Rajabioun, 2011):

Stage 1: We'll randomly specify where the cuckoos are staying.

Stage 2: Distribute eggs among the cuckoos.

Stage 3: Calculate how far apart each cuckoo nest is.

Stage 4: The egg-laying by the cuckoo in the host bird's nest.

Stage 5: If host birds find eggs, they will be destroyed.

Stage 6: An incubator is used to grow eggs that have yet to be recognized.

Stage 7: Evaluate the cuckoos' new home.

Stage 8: After the maximum number of cuckoos for a specific area has been established, any cuckoos found in the wrong locations will be removed.

Stage 9: Cuckoos are sorted into groups using the k-means algorithm. The optimal cuckoo cluster is selected as the destination.

Stage 10: Transport the newly established cuckoo population to the designated area.

Stage 11: Verify the stop condition; if it has not been set, go to Step 2.

Production of cuckoo nesting areas (initial population solutions)

The habitat in this approach is an array whose elements are the values of the problem variables. The following is an example definition of a habitat for a *D*-dimensional optimization problem:

$$HabitatorX_i = [x_1, x_2, \ldots, x_D] \quad (17)$$

The degree of suitability (or amount of profit) in the current habitat is obtained by evaluating the profit function f in the habitat:

$$f(HabitatorX_i) = f([x_1, x_2, \ldots, x_D]) \quad (18)$$

It is sufficient to increase the cost function by a negative sign to use COA when finding solutions to minimization situations. Each of these environments is given a certain number of eggs to work with. In the wild, a cuckoo will lay anywhere from 5 to 20 eggs in one location. Throughout several iterations, these values are utilized to determine the top and lower boundaries of the egg allotment given to each cuckoo.

The maximum laying range, also known as *ELR*, is a function of several factors, including the total number of eggs, the present number of cuckoo eggs, and the upper and lower bounds of the issue variables. In light of this, the *ELR* may be understood to refer to the following relationship:

$$ELR = \sigma \times \frac{\text{Number of current cuckoos eggs}}{\text{Tota l number of eggs } (Xmin_{max})} \tag{19}$$

σ The setting factor of the maximum radius is *ELR*.

Cuckoos have been seen to nest in the ELR of the host bird.

Then, after each round of egg-laying, the *p*% of eggs (often 10%) with the lowest objective function value or profit is destroyed.

Cuckoo habitats

K-means classification puts the cuckoos into groups, and *k*-values between 3 and 5 are generally enough. We can determine where a given community would be best served by averaging everyone's aims. Then the group whose average value of the goal function or profit is most significant is chosen as the target, and the other groups begin to move in that direction. Each cuckoo in this migration takes a detour φ from the best possible route, covering just δ% of the total distance between the origin and destination.

The cuckoo can better investigate its surroundings with these two variables. An angle φ between -π/6 and π/6, and δ a random value between 0 and 1, respectively. When all the cuckoos have arrived at their destination, and their new homes have been identified, they will each have a clutch of eggs. Each cuckoo is assigned an *ELR* based on its egg production, and laying starts afterward. The cuckoo optimization method uses a migration operator defined by the following formula:

$$X_i^{new} = X_i + F \times (X_{best} - X_i) \tag{20}$$

The parameter determines the level of divergence, denoted by *F*, and *Xbest* indicates the best solution the algorithm has produced to this point.

To keep the population from fluctuating too much, a maximum number of cuckoos, or algorithms, known as *Nmax*, has been established. If the cuckoo population surpasses this barrier, any birds found to be residing in areas where they are not welcome will be eradicated.

Convergent optimization with the use of COA

This method repeats itself until all cuckoo populations have the highest possible degree of egg likeness to their host birds and are situated such that they are close to the greatest number of food sources. This position will optimize revenues, or the function sought while lowering the number of eggs harmed.

3.2 The proposed method

The Cuckoo search algorithm has been updated to make local searches more effective in terms of their efficiency. In practice, the solutions in the COA move very quickly toward *Xbest* and a position equal to what they obtain with X_{best}. In other words, they become trapped in the optimal local solution, and the COA loses its ability to optimize, as shown by equation (20) and the simulations performed in this article. In addition, the COA loses its optimization power. Because of this, it is necessary to improve the algorithm's capability to do local searches. Because of this, we have suggested the usage of a new operator in the fundamental movement equation of the cuckoo optimization strategy. This operator is written as $-rand*(X_{worst}-X_i)$. Whenever members of the population move very quickly to the X_{best} value and the value of $(X_{best} - X_i)$ tends to zero, the new operator $-rand*(X_{worst} - X_i)$ tends to zero much more slowly due to the utilization of X_{worst}. This is the case regardless of whether the value of $(X_{best} - X_i)$ tends to zero. Therefore, members keep up their efforts to search and migrate around the country in the expectation that the outcomes of our simulation will illustrate the efficacy of the new search vector in the proper context. The *F* parameter of the modified COA (MCOA) is removed in favor of a random integer in this method, which reduces the technique's overall complexity. The migration operator formula may be represented as a relation when using the modified cuckoo optimization approach, which is as follows:

$$X_i^{new} = X_i + rand \times (X_{best} - X_i) - rand \times (X_{worst} - X_i) \quad (21)$$

Here, *rand* represents the random values are numbers between 0 and 1.

3.3. Time Complexity

It is worthwhile to remember that MCOA's computational complexity is determined by three processes: initialization, fitness evaluation, and updating of the algorithm population. Consequently, the computational complexity of the initialization process is *O*(*Npop*). As a result, the computational complexity of the updating mechanism is *O*(*Itermax* + *Npop*)+*O*(*Itermax* + *Npop* + *D*), in which the aim is to find the most optimal location and update the location vector of all populations. The maximum number of iterations *itermax* is determined by the dimension of the problem, and *D* is the maximum number of iterations. MCOA, like the original COA algorithm, has a computational complexity of *O*(*Npop*×(*Itermax* + *Itermax* ×*D* + 1)).

4. MCOA for Solving the Various OPF Problems in the IEEE standard 30-bus system

In this section, the proposed MCOA algorithm is implemented in MATLAB 2014a. And for load distribution analysis, MATPOWER (Zimmerman et al., n.d.) software is used. All cases are executed on the IEEE standard 30-bus system (Mohamed et al., 2017), which is used in many articles, as shown in Figure 1. For all investigated cases, a population of 60 and a number of repetitions of 400 were used in both COA and MCOA algorithms. In order to make the proposed MCOA method effective and compare it with COA, eight OPF scenarios have been considered and simulated.

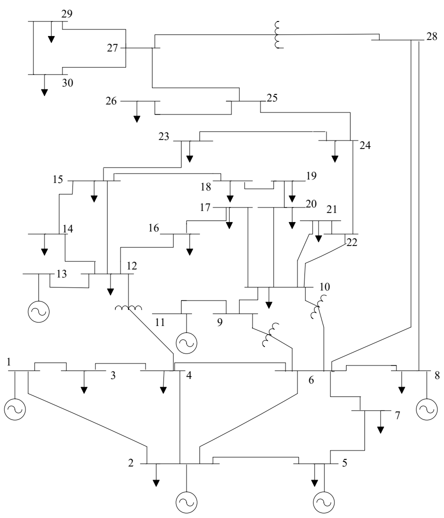

Figure 1: The layout of the IEEE 30-bus network.

In the supplemental material, Table 1 summarizes MCOA's conclusive findings for the 30-bus power system under six different OPF scenarios that do not use stochastic renewable energy.

Table 1:The ideal values for the variables that MCOA found for OPF without using stochastic renewable energy.

Var.	Cases					
	1	2	3	4	5	6
PG1 (MW)	177.1373	140.0000	198.7757	102.6071	175.5192	122.1789
PG2	48.7211	55.0000	44.7459	55.5533	48.4117	52.5609
PG5	21.3808	24.1481	18.5791	38.1102	21.2771	31.4833
PG8	21.2481	34.9526	10.0000	35.0000	23.1580	35.0000
PG11	11.9338	19.2642	10.0002	30.0000	12.8093	26.7244
PG13	12.0001	16.7568	12.0000	26.6587	12.0000	21.0401
VG1 (p.u.)	1.0836	1.0757	1.0807	1.0698	1.0429	1.0732
VG2	1.0605	1.0581	1.0573	1.0576	1.0225	1.0574
VG5	1.0339	1.0324	1.0296	1.0359	1.0152	1.0325
VG8	1.0382	1.0410	1.0360	1.0438	1.0041	1.0407
VG11	1.0999	1.0810	1.0969	1.0834	1.0723	1.0401
VG13	1.0511	1.0561	1.0710	1.0573	0.9902	1.0246
T6–9	1.0782	1.0229	1.0987	1.0744	1.0972	1.0997
T6–10	0.9057	0.9611	0.9002	0.9111	0.9017	0.9509
T4-12	0.9787	0.9917	1.0040	0.9901	0.9399	1.0331
T28–27	0.9729	0.9737	0.9772	0.9750	0.9693	1.0046
QC10 (MVAR)	1.1748	4.9159	5.0000	4.6868	4.5850	3.1626
QC12	2.3807	3.3019	0.0029	0.1790	0.0289	0.0401
QC15	4.2578	4.1233	4.9995	4.4675	4.7603	3.8335
QC17	4.9792	5.0000	4.9941	5.0000	0.2594	4.9998
QC20	4.2860	4.4169	0.0	4.2431	4.9959	4.9997
QC21	4.9980	4.9918	4.9999	5.0000	4.7559	5.0000
QC23	3.3965	3.6741	3.5363	3.2614	4.9780	4.2152
QC24	4.9973	4.9986	5.0000	5.0000	4.9766	5.0000
QC29	2.6408	2.6782	2.7027	2.5507	2.7285	2.6110
Cost ($/h)	800.4791	646.4890	832.2134	859.0154	803.7176	830.2798
Emission (t/h)	0.3663	0.2835	0.4379	0.2289	0.3614	0.2529
Power losses (MW)	9.0212	6.7217	10.7009	4.5263	9.7753	5.5876
V.D. (p.u.)	0.9091	0.9277	0.8323	0.9298	0.0941	0.2971

4.1 Case 1: Minimizing the fuel cost

Several aspects of the objective function were considered while working on the OPF issue for this research. The first component of this goal function of minimizing fuel costs is resources, which is the same as the conventional cost function in that it has the same meaning.

$$J_1 = \sum_{i=1}^{NG} (\alpha_i + b_i P_{Gi} + c_i P_{Gi}^2) \qquad (22)$$

where the coefficients a_i, *bi,* and c_i (Mohamed et al., 2017) show the costs associated with the *i*th unit.

Table 2 compares testified findings from recent works such as MSA (Mohamed et al., 2017), MGBICA (Ghasemi, Ghavidel, Ghanbarian, et al., 2015), MRFO (Guvenc et al., 2020), MPSO-SFLA (Narimani et al., 2013), EP (SOOD, 2007), IEP (Ongsakul & Tantimaporn, 2006), PSOGSA (Radosavljević et al., 2015), GWO (Niknam, Narimani, Aghaei, et al., 2011), FPA (Mohamed et al., 2017), ARCBBO (Ramesh Kumar & Premalatha, 2015), JAYA (Warid et al., 2016), MICA-TLA (Ghasemi, Ghavidel, Rahmani, et al., 2014), PPSOGSA (Ullah et al., 2019), DE (Sayah & Zehar, 2008), MHBMO (El-Fergany & Hasanien, 2015), MFO (Mohamed et al., 2017), TS (Abido, 2002), AGSO (Hazra & Sinha, 2011), SFLA-SA (Niknam, Narimani, Jabbari, et al., 2011), SKH (Pulluri et al., 2018), ABC (Abaci & Yamacli, 2016), and AO (Khamees et al., 2021) on the OPF of COA and MCOA algorithms.

According to Table 2, the provided algorithm outperformed the others in attaining the lowest potential fuel cost. The convergence properties of the COA and MCOA algorithms are shown in Figure 2. From this diagram, it is easy to see that in case 1, the algorithms reach a correct final solution at the right moment.

Table 2: The optimal solutions for case 1.

Optimizer	Fuel cost ($/h)	Emission (t/h)	Power losses (MW)	V.D. (p.u.)
MSA (Mohamed et al., 2017)	800.5099	0.36645	9.0345	0.90357
MGBICA (Ghasemi, Ghavidel, Ghanbarian, et al., 2015)	801.1409	0.3296	-	-
MRFO (Guvenc et al., 2020)	800.7680	-	9.1150	-
MPSO-SFLA (Narimani et al., 2013)	801.75	-	9.54	-
EP (SOOD, 2007)	803.57	-	-	-
IEP (Ongsakul & Tantimaporn, 2006)	802.46	-	-	-
PSOGSA (Radosavljević et al., 2015)	800.49859	-	9.0339	0.12674

GWO (Niknam, Narimani, Aghaei, et al., 2011)	801.41	-	9.30	-
FPA (Mohamed et al., 2017)	802.7983	0.35959	9.5406	0.36788
ARCBBO (Ramesh Kumar & Premalatha, 2015)	800.5159	0.3663	9.0255	0.8867
JAYA (Warid et al., 2016)	800.4794	-	9.06481	0.1273
MICA-TLA (Ghasemi, Ghavidel, Rahmani, et al., 2014)	801.0488	-	9.1895	-
PPSOGSA (Ullah et al., 2019)	800.528	-	9.02665	0.91136
DE (Sayah & Zehar, 2008)	802.39	-	9.466	-
MHBMO (El-Fergany & Hasanien, 2015)	801.985	-	9.49	-
MFO (Mohamed et al., 2017)	800.6863	0.36849	9.1492	0.75768
TS (Abido, 2002)	802.29	-	-	-
AGSO (Hazra & Sinha, 2011)	801.75	0.3703	-	-
SFLA-SA (Niknam, Narimani, Jabbari, et al., 2011)	801.79	-	-	-
SKH (Pulluri et al., 2018)	800.5141	0.3662	9.0282	-
ABC (Abaci & Yamacli, 2016)	800.660	0.365141	9.0328	0.9209
AO (Khamees et al., 2021)	801.83	-	-	-
COA	801.7449	0.3739	9.4432	0.5715
MCOA	800.4791	0.3663	9.0212	0.9091

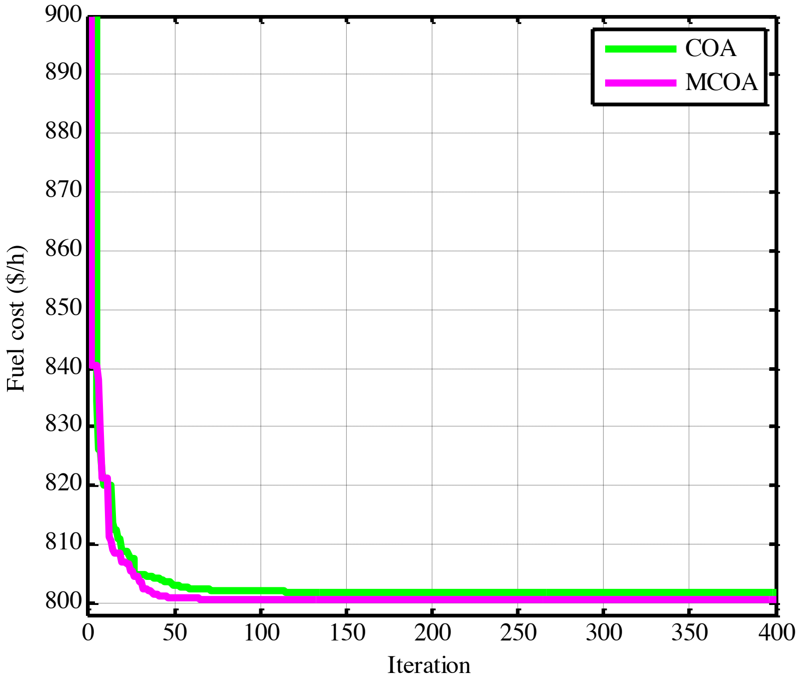

Figure 2: Convergence for case 1.

4.2 Case 2: Minimizing piecewise quadratic fuel cost functions.

Thermal generators can operate on a wide range of fuels depending on the requirements of the network. Consequently, we may consider the theoretical analysis of the F curve for these units (1 and 2) to be a collection of constraints.

$$F(P_{Gi}) = \begin{cases} \alpha_{i1} + c_{i1}P_{Gi}^2 + b_{i1}P_{Gi} & P_{Gi}^{\min} \le P_{Gi} \le P_{Gi1} \\ \ldots & \\ \alpha_{ik} + c_{ik}P_{Gi}^2 + b_{ik}P_{Gi} & P_{Gik-1} \le P_{Gi} \le P_{Gi}^{\max} \end{cases} \quad (23)$$

For the kth kind of fuel, the cost coefficients of generator i are indicated by the notation a_{ik}, b_{ik}, and $c_{ik,}$ respectively.

As a direct consequence of this, the goal function for modeling the features of fuel costs may be shown as follows:

$$J_2 = \left(\sum_{i=1}^{NG} \alpha_{ik} + c_{ik}P_{Gi}^2 + b_{ik}P_{Gi} \right) \quad (24)$$

Table 3 compares these results to the outcomes that have been reported in the most recent research, such as MDE (Sayah & Zehar, 2008), MPSO-SFLA (Narimani et al., 2013), MSA (Mohamed et al., 2017), IEP (Ongsakul & Tantimaporn, 2006), SSA (Jebaraj & Sakthivel, 2022), SSO (Nguyen, 2019), GABC (Roy & Jadhav, 2015), FPA (Mohamed et al., 2017), MICA-TLA (Ghasemi, Ghavidel, Rahmani, et al., 2014), MFO (Mohamed et al., 2017), and LTLBO (Ghasemi, Ghavidel, Gitizadeh, et al., 2015). The fuel that costs the least per hour ($/h), produces the fewest emissions ($/ton), wastes the least amount of power (MW), and has the lowest *V.D.* (p.u.) is the one that wins. This table demonstrates that the MCOA approach described here performs better than the other algorithms that were taken into consideration. Figure 3 illustrates the convergence characteristic curve of the two algorithms that were investigated for this work to find the optimum solution.

Table 3: The optimal solutions for case 2.

Optimizer	Fuel cost ($/h)	Emission (t/h)	Power losses (MW)	V.D. (p.u.)
MDE (Sayah & Zehar, 2008)	647.846	-	7.095	-
MPSO-SFLA (Narimani et al., 2013)	647.55	-	-	-
MSA (Mohamed et al., 2017)	646.8364	0.28352	6.8001	0.84479
IEP (Ongsakul & Tantimaporn, 2006)	649.312	-	-	-
SSA (Jebaraj & Sakthivel, 2022)	646.7796	0.2836	6.5599	0.5320
SSO (Nguyen, 2019)	663.3518	-	-	-
GABC (Roy & Jadhav, 2015)	647.03	-	6.8160	0.8010
FPA (Mohamed et al., 2017)	651.3768	0.28083	7.2355	0.31259
MICA-TLA (Ghasemi, Ghavidel, Rahmani, et al., 2014)	647.1002	-	6.8945	-
MFO (Mohamed et al., 2017)	649.2727	0.28336	7.2293	0.47024
LTLBO (Ghasemi, Ghavidel, Gitizadeh, et al., 2015)	647.4315	0.2835	6.9347	0.8896
COA	649.8857	0.2824	7.4359	0.6474
MCOA	646.4890	0.2835	6.7217	0.9277

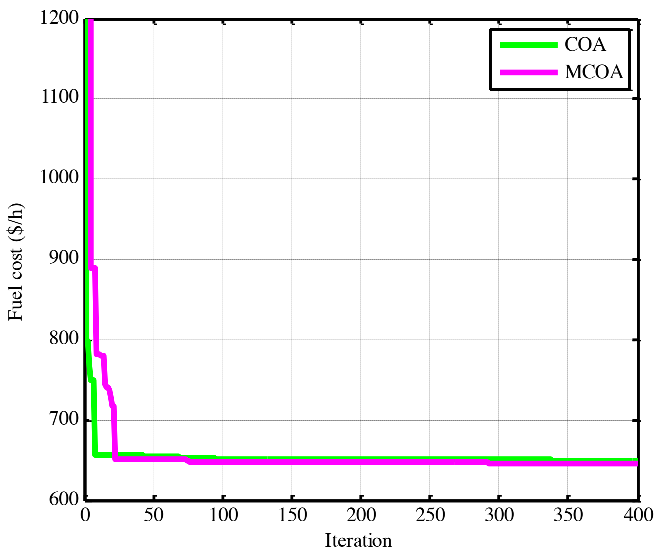

Figure 3: Convergence for case 2.

4.3 Case 3: Considering valve point effects (VPEs)

The quadratic cost function achieves a higher degree of accuracy and realism as a direct result of the influence of tap point loading. When steam is introduced, the valves on thermal generating units open, which results in rapid increases in losses and causes ripples in the cost function curve. This causes VPEs. The effect of this is that the cost function may be expressed as follows (Biswas et al., 2018):

$$J_3 = \sum_{i=1}^{NG} \left| d_i \sin\left(e_i \left(P_{Gi}^{\min} - P_{Gi}\right)\right) \right| + \sum_{i=1}^{NG} \alpha_i + b_i P_{Gi} + c_i P_{Gi}^2 \tag{25}$$

where d_i and e_i are the ith generator's price and efficiency factors (Biswas et al., 2018).

Results from SP-DE (Biswas et al., 2018), PSO (Bouchekara et al., 2016), COA, and MCOA algorithms are shown in Table 4. It is clear from the data presented in this table that the MCOA is an algorithm that is well-suited to the complex OPF. It is also clear from the algorithm convergence graph in Figure 4 that the MCOA can achieve good and acceptable optimal solutions.

Table 4: The optimal solutions for case 3.

Optimizer	Fuel cost ($/h)	Emission (t/h)	Power losses (MW)	V.D. (p.u.)
COA	832.8498	0.4390	10.9273	0.7216
MCOA	832.2134	0.4379	10.7009	0.8323
SP-DE (Biswas et al., 2018)	832.4813	0.43651	10.6762	0.75042
PSO (Bouchekara et al., 2016)	832.6871	-	-	-

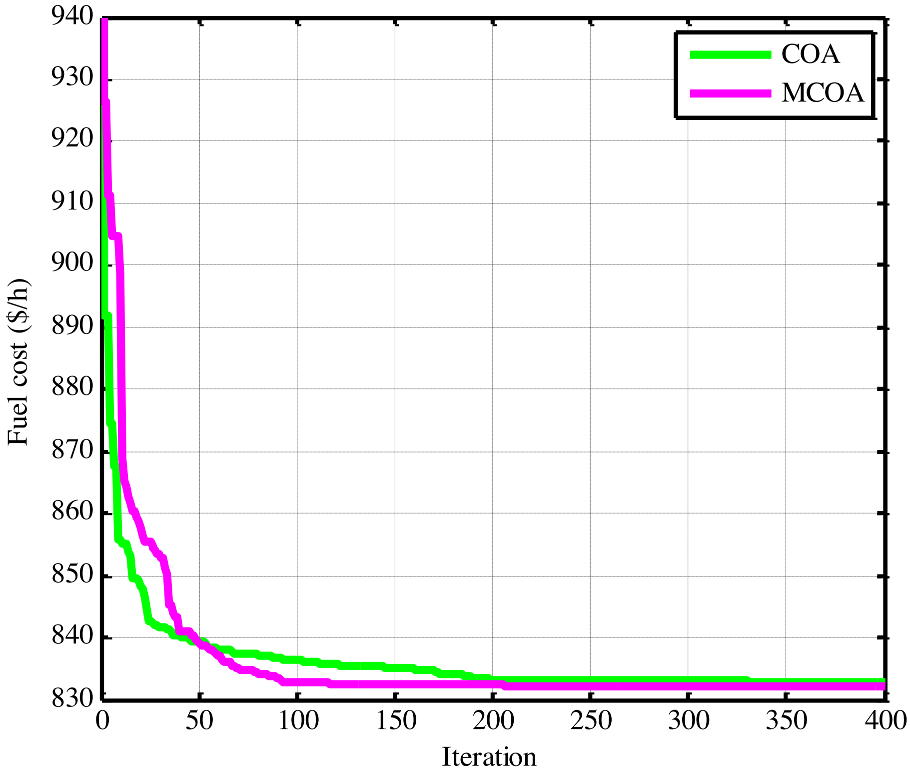

Figure 4: Convergence for case 3.

4.4 Case 4: Minimizing the fuel cost and real power loss

Engineers strive to minimize energy loss in the transmission of electricity. Therefore, we want to lessen network fuel and losses in this case. The correct form of the objective function is as follows:

$$J_4 = \lambda p * P_{Loss} + J_1 \qquad (26)$$

The value of factor λp has been chosen as equal to 40 (Biswas et al., 2018).

Network loss (P_{Loss}) can be modeled as the following average (Biswas et al., 2018):

$$P_{Loss} = \sum_{\substack{k=1 \\ k=(i,j)}}^{NTL} g_k (V_i^2 + V_j^2 - 2\, V_i V_j \cos \delta_{ij}) \qquad (27)$$

As seen above, the conductance of the kth branch is denoted by the symbol g_k.

In Table 5, we provide the optimal answers to this instance, as determined by the algorithms explored in this research and the techniques analyzed in the relevant prior literature. The results show that the approach put forth in this MCOA paper is the best option. Figure 5 below displays the convergence characteristics of the examined methods for the top 30 run-average solutions.

Table 5: The optimal solutions for case 4.

Optimizer	Fuel cost ($/h)	Emission (t/h)	Power losses (MW)	V.D. (p.u.)	J_4
SF-DE (Biswas et al., 2018)	859.1458	0.2289	4.5245	0.92731	1040.1258
MJaya (Warid et al., 2018)	827.9124	-	5.7960	-	1059.7524
QOMJaya (Warid et al., 2018)	826.9651	-	5.7596	-	1402.9251
EMSA (Bentouati et al., 2020)	859.9514	0.2278	4.6071	0.7758	1044.2354
MOALO (Herbadji et al., 2019)	826.4556	0.2642	5.7727	1.2560	1057.3636
SpDEA (Ghoneim et al., 2021)	837.8510	-	5.6093	0.8106	1062.223
MSA (Mohamed et al., 2017)	859.1915	0.2289	4.5404	0.92852	1040.8075
COA	859.2413	0.2291	4.5359	0.9113	1040.6773
MCOA	859.0154	0.2289	4.5263	0.9298	1040.0674

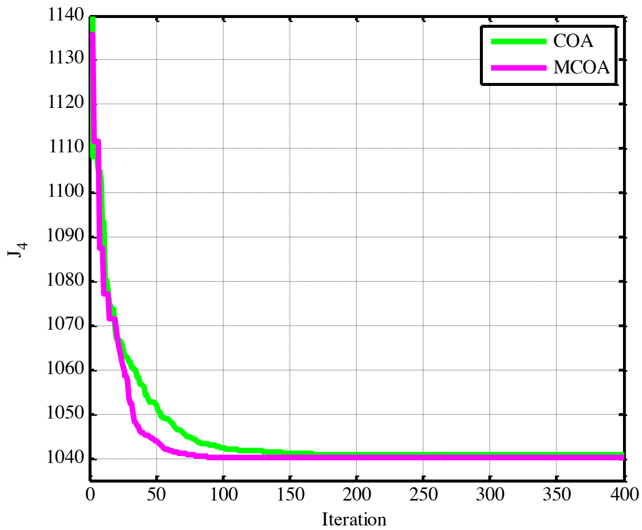

Figure 5: Convergence for case 4.

4.5 Case 5: Minimizing the fuel cost and voltage deviation.

The voltage specification is the most important of all the factors considered when determining a network's dependability. This may be modified by reducing the voltage gap between the load and the bus to a value closer to unity. An acceptable solution is found when the cost alone is used as the target function; however, the voltage variations associated with this solution are undesirable. Therefore, the objective function of the optimum load distribution in scenario 5 of this article is described below to minimize both voltage deviations (V.D.) and fuel costs.

$$J_5 = \lambda v * \sum_{i=1}^{NPQ} |V_i - 1.0| + J_1 \qquad (28)$$

where the value of the component λv is set to 100 (Biswas et al., 2018).

Table 6 presents the best results that could be achieved for case 5 using the techniques discussed in this article, as well as findings from more recent investigations. MCOA has produced the lowest and best values for this objective function in comparison to other approaches shown in Table 6. Figure 6 presents the characteristic convergence curves of the various methods.

Table 6: The optimal solutions for case 5.

Optimizer	Fuel cost ($/h)	Emission (t/h)	Power losses (MW)	V.D. (p.u.)	J_5
BB-MOPSO (Ghasemi, Ghavidel, Ghanbarian, et al., 2014)	804.9639	-	-	0.1021	815.1739
DA-APSO (Shilaja & Ravi, 2017)	802.63	-	-	0.1164	814.2700
SpDEA (Ghoneim et al., 2021)	803.0290	-	9.0949	0.2799	831.0190
MNSGA-II (Ghasemi, Ghavidel, Ghanbarian, et al., 2014)	805.0076	-	-	0.0989	814.8976
PSO-SSO (El Sehiemy et al., 2020)	803.9899	0.367	9.961	0.0940	813.3899
SSO (El Sehiemy et al., 2020)	803.73	0.365	9.841	0.1044	814.1700
PSO (El Sehiemy et al., 2020)	804.477	0.368	10.129	0.126	817.0770
MFO (Mohamed et al., 2017)	803.7911	0.36355	9.8685	0.10563	814.3541
EMSA (Bentouati et al., 2020)	803.4286	0.3643	9.7894	0.1073	814.1586
TFWO (Sarhan et al., 2022)	803.416	0.365	9.795	0.101	813.5160
ECHT-DE (Biswas et al., 2018)	803.7198	0.36384	9.8414	0.09454	813.1738
MOMICA (Ghasemi, Ghavidel, Ghanbarian, et al., 2014)	804.9611	0.3552	9.8212	0.0952	814.4811
MPSO (Mohamed et al., 2017)	803.9787	0.3636	9.9242	0.1202	815.9987
COA	804.0138	0.3673	10.0020	0.1071	814.7277
MCOA	803.7176	0.3614	9.7753	0.0941	813.1276

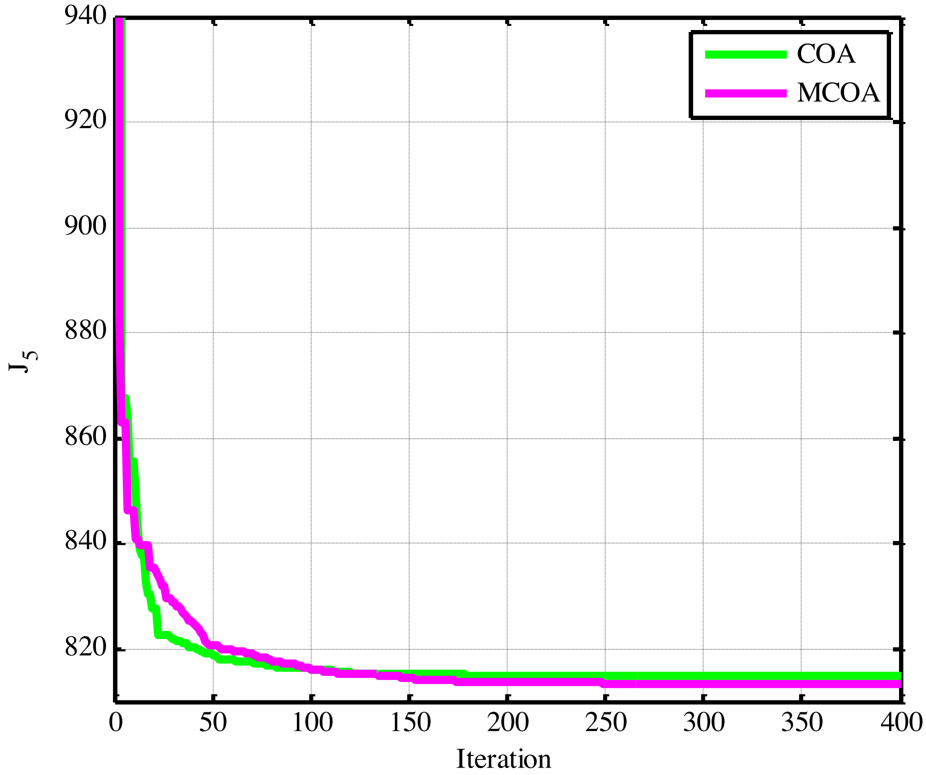

Figure 6: Convergence for case 5.

4.6 Case 6: Minimizing the fuel cost, voltage deviation, emissions, and losses

This function models fuel cost, voltage deviation, active power loss and emission with λv = 21, λp = 22 and λe = 19 (Biswas et al., 2018):

$$J_6 = J_1 + \lambda v * \sum_{i=1}^{NPQ} |V_i - 1.0| + \lambda e * \sum_{i=1}^{NG} F_{Ei}(P_{Gi}) + \lambda p * P_{Loss} \quad (29)$$

$\sum_{i=1}^{NG} F_{Ei}(P_{Gi})$ is expressed as follows:

$$F_E = \sum_{i=1}^{NG} \left(\alpha_i + \xi_i \, exp(\lambda_i P_{Gi}) + \beta_i P_{Gi} + \gamma_i P_{Gi}^2\right) \quad (30)$$

where F_{Ei} signifies the emission,γ_i,β_i, ξ_i and λ_i show the emission coefficients of ith generator.

Table 7 summarizes the findings of the algorithms investigated in this study compared to the most successful results of more recent papers. This table makes it abundantly evident that the MCOA optimization technique is the superior choice among these other optimization approaches for the sixth ideal load distribution scenario. Figure 7 depicts, after that, the convergence characteristic of the COA and MCOA algorithms used in this example.

Table 7: The optimal solutions for case 6.

Algorithm	Fuel cost ($/h)	Emission (t/h)	Power losses (MW)	V.D. (p.u.)	J_6
MSA (Mohamed et al., 2017)	830.639	0.25258	5.6219	0.29385	965.2907
SSO (El Sehiemy et al., 2020)	829.978	0.25	5.426	0.516	964.9360
PSO (El Sehiemy et al., 2020)	828.2904	0.261	5.644	0.55	968.9674
J-PPS3 (Gupta et al., 2021)	830.3088	0.2363	5.6377	0.2949	965.0228
J-PPS2 (Gupta et al., 2021)	830.8672	0.2357	5.6175	0.2948	965.1201
J-PPS1 (Gupta et al., 2021)	830.9938	0.2355	5.6120	0.2990	965.2159
MNSGA-II (Ghasemi, Ghavidel, Ghanbarian, et al., 2014)	834.5616	0.2527	5.6606	0.4308	972.9429
MFO (Mohamed et al., 2017)	830.9135	0.25231	5.5971	0.33164	965.8080
MOALO (Herbadji et al., 2019)	826.2676	0.2730	7.2073	0.7160	1005.0512
MODA (Ouafa et al., 2017)	828.49	0.265	5.912	0.585	975.8740
I-NSGA-III (Zhang et al., 2019)	881.9395	0.2209	4.7449	0.1754	994.2078
BB-MOPSO (Ghasemi, Ghavidel, Ghanbarian, et al., 2014)	833.0345	0.2479	5.6504	0.3945	970.3379
COA	830.2933	0.2558	5.7225	0.3319	968.0184
MCOA	830.2798	0.2529	5.5876	0.2971	964.2521

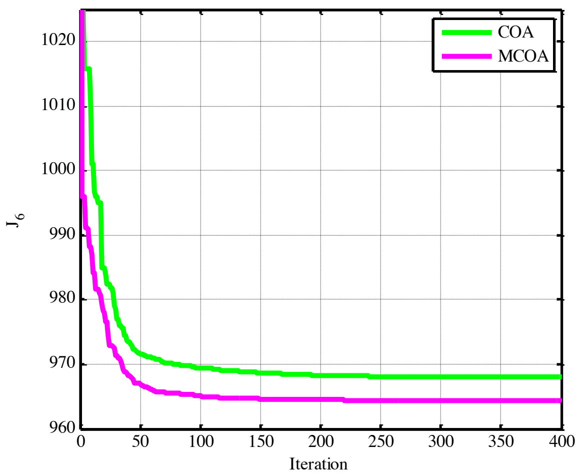

Figure 7: Convergence for case 6.

4.7 OPF solutions, including stochastic solar and wind power.

Wind Power

In order to construct a work optimization strategy to deal with OPF challenges, a future wind energy profile prediction is required. These forecasts are calculated with the use of the Weibull probability distribution function. The first stage in finding a solution to a problem is to estimate how much energy can be generated from the wind, which may be done independently. Wind speed is a common input into models of wind power generation. Here, the Weibull probability distribution function is used to create and simulate the wind speed $f_v(v)$, where k and c are dimensionless form factors and step sizes, respectively, in the following equations (Biswas et al., 2018):

$$f_v(v) = \frac{k}{c}\left(\frac{v}{c}\right)^{k-1} \times e^{-\left(\frac{v}{c}\right)^k} \tag{31}$$

According to formula (33), [22] the average of the Weibull probability distribution (M_{wbl}) is mainly determined by $\Gamma(x)$ (32) (Biswas et al., 2018):

$$M_{wbl} = c * \Gamma(1 + K^{-1}) \tag{32}$$

$$\Gamma(x) = \int_0^{\infty} e^{-t} t^{x-1} dt \tag{33}$$

A wind turbine is a device that generates electricity from the kinetic and potential energy of the wind. The relation between wind velocity and the electrical power generated by a wind turbine is given by equation (34) (Biswas et al., 2018).

$$P_w(v) = \begin{cases} 0;\ v \le v_{in} \text{and} v > v_{out} \\ P_{wr}\left(\frac{v - v_{in}}{v_r - v_{in}}\right);\ v_{in} < v \le v_r \\ P_{wr};\ v_r < v \le v_{out} \end{cases} \tag{34}$$

where P_{wr} is the wind turbine's rated power, wind turbine's cut-in wind rate is v_{in}, and v_{out} is the cut-out wind rate and v_r is the valued wind speed.

Equation (43) describes the total cost of wind power generation in (USD/h), which includes three main items: direct wind turbine, storage, and penalty costs (Biswas et al., 2018).

$$C_W^T = \sum_{j=1}^{N_W}\left[C_{w,j}(P_{ws,j}) + C_{Pw,j}(P_{wav,j} - P_{ws,j}) + C_{Rw,j}(P_{ws,j} - P_{wav,j})\right] \tag{35}$$

Suppose the power production from the wind turbine is less than the value anticipated. In that case, a storage charge will be levied to compensate for the forecasted value. A fine is imposed on the company if the actual consumption of wind energy is higher than the predicted figure. Because of this, having a system that provides an accurate assessment of the wind power profile is of the utmost importance. The costs are broken down into USD per hour using the methodology outlined in (Biswas et al., 2018).

Solar power units

It is difficult to forecast how much energy can be harvested from the sun because of atmospheric variables like clouds and solar radiation. Since solar radiation is a known quantity, it may be used to calculate the maximum power generated by solar systems (G).

In this section, the lognormal probability distribution function $f_G(G)$(Biswas et al., 2018):

$$f_G(G) = \frac{k}{G\sigma\sqrt{2\pi}} \times e^{-\left(\frac{(\ln x - \mu)}{2\sigma^2}\right)} \text{ for } G>0 \tag{36}$$

The conversion of solar energy into usable power is the final goal of a solar energy system.

In equation (36), the estimated solar radiation is utilized to describe the output power of this system, which is denoted by the function $P_s(G)$ as a function (Biswas et al., 2018):

$$P_s(G) = \begin{cases} P_{sr}\frac{G^2}{G_{std}R_c};\ 0 < G < R_c \\ P_{sr}\frac{G}{G_{std\,c}};\ G \ge R_c \end{cases} \tag{37}$$

The cost of producing energy from solar sources is broken down into three distinct categories, much as the cost of producing electricity from wind sources, to mitigate the effects of the inherent uncertainty in the cost estimate.

Equation (38) determine the following sum of all components in terms of their respective (USD/h) values (Biswas et al., 2018):

$$C_S^T = \sum_{k=1}^{N_S} \left[C_{s,j}\left(P_{ss,k}\right) + C_{Rs,k}\left(P_{ss,k} - P_{sav,k}\right) + C_{Ps,k}\left(P_{sav,k} - P_{ss,k}\right) \right] \quad (38)$$

wind/solar integrated OPF constraints and variables

To incorporate the variables associated with the wind and solar power generations into the conventional OPF problem, some modifications and additional constraints should be considered. So, the equality constraints (6) and (7) are expressed as given in (39) and (40).

$$P_{Gi} + P_{ws,i} + P_{ss,i} - P_{Di} - V_i \sum_{j=1}^{NB} V_j \left[B_{ij} \sin\ (\delta_i - \delta_j) + G_{ij} \cos\ (\delta_i - \delta_j) \right] = 0 \quad (39)$$

$$Q_{Gi} + Q_{ws,i} + Q_{ss,i} - Q_{Di} - V_i \sum_{j=1}^{NB} V_j \left[G_{ij} \sin(\delta_i - \delta_j) - B_{ij} \cos(\delta_i - \delta_j) \right] = 0 \quad (40)$$

Also, the voltage magnitude, active and reactive power generations at the installed locations of the wind and solar power generation units are restricted using the constraints (41) to (46).

$$V_{ws,i}^{min} \le V_{ws,i} \le V_{ws,i}^{max} \quad (41)$$

$$P_{ws,i}^{min} \le P_{ws,i} \le P_{ws,i}^{max} \quad (42)$$

$$Q_{ws,i}^{min} \le Q_{ws,i} \le Q_{ws,i}^{max} \quad (43)$$

$$V_{ss,i}^{min} \le V_{ss,i} \le V_{ss,i}^{max} \quad (44)$$

$$P_{ss,i}^{min} \le P_{ss,i} \le P_{ss,i}^{max} \quad (45)$$

$$Q_{ss,i}^{min} \le Q_{ss,i} \le Q_{ss,i}^{max} \quad (46)$$

In the wind/solar integrated OPF problem, the control variables, u is defined as follows:

$$\begin{aligned} u &= [Q, V_G, V_W, V_S, P_W, P_S, P_G, T], \\ Q &= [Q_{C_1}, \dots, Q_{C_{NC}}], \\ V_G &= [V_{G_1}, \dots, V_{G_{NG}}], \\ V_W &= [V_{ws,1}, \dots, V_{ws,N_W}], \\ V_S &= [V_{ss,1}, \dots, V_{ss,N_S}], \\ P_W &= [P_{ws,1}, \dots, P_{ws,N_W}], \\ P_S &= [P_{ss,1}, \dots, P_{ss,N_S}], \\ P_G &= [P_{G_2}, \dots, P_{G_{NG}}], \\ T &= [T_1, \dots, T_{NT}]. \end{aligned} \quad (47)$$

Besides, the state variables, x is represented as follows:

$$\begin{aligned} x &= [S, Q_W, Q_S, Q_G, V_l, P_{G_1}], \\ S &= [S_{l_1}, \dots, S_{l_{NTL}}], \\ Q_W &= [Q_{ws,1}, \dots, Q_{ws,N_W}], \\ Q_s &= [Q_{ss,1}, \dots, Q_{ss,N_S}], \\ Q_G &= [Q_{G_1}, \dots, Q_{G_{NG}}], \\ V_l &= [P_{ws,1}, \dots, P_{ws,N_W}]. \end{aligned} \quad (48)$$

4.7.1 Case 7: Minimizing generation costs considering the variable nature of renewable sources

According to (39), case 7 minimizes and maximizes the overall cost of generating electricity by thermal and renewable energy sources (Biswas et al., 2018). The PDF parameters are outlined in (Biswas et al., 2018), and the cost coefficients are unchanged from case 1.

$$\begin{aligned} J_7 = J_1 &+ \sum_{k=1}^{N_S} \left[C_{s,j}\left(P_{ss,k}\right) + C_{Ps,k}\left(P_{sav,k} - P_{ss,k}\right) + C_{Rs,k}\left(P_{ss,k} - P_{sav,k}\right) \right] \\ &+ \sum_{j=1}^{N_W} \left[C_{w,j}\left(P_{ws,j}\right) + C_{Pw,j}\left(P_{wav,j} - P_{ws,j}\right) + C_{Rw,j}\left(P_{ws,j} - P_{wav,j}\right) \right] \end{aligned} \quad (49)$$

Table 8 displays the best possible answers obtained from each algorithm tested in this research after 30 iterations. P_{ws1} shows the expected output from W_{G1}, and so on, for each successive wind generator. According to this table, the proposed MCOA algorithm has successfully located optimal solutions that are both of a higher quality and perform much better than the original COA approach. The convergent behavior of the two algorithms is shown in Figure 8 for case 7 of the research.

Table 8: The optimal variables for case 7.

Variables	COA	MCOA
PG1 (MW)	134.90794	134.90791
PG2 (MW)	27.5907	27.7283
Pws1 (MW)	43.1839	43.3109
PG3 (MW)	10.0001	10
Pws2 (MW)	36.2407	36.5707
Pss (MW)	37.2677	36.6646
VG1 (p.u.)	1.0717	1.0721
VG2 (p.u.)	1.0567	1.0571
VG5 (p.u.)	1.0346	1.035
VG8 (p.u.)	1.0396	1.0397
VG11 (p.u.)	1.0992	1.0983
VG13 (p.u.)	1.0587	1.0551
QG1 (MVAR)	-2.12274	-1.95067
QG2 (MVAR)	12.4535	13.2051
Qws1 (MVAR)	23.1089	23.2034
QG3(MVAR)	34.7495	35.0095
Qws2 (MVAR)	30	30
Qss (MVAR)	18.8345	17.5462
Fuelvlvcost ($/h)	437.5577	438.0114
Wind gen cost ($/h)	241.8954	243.4495
Solar gen cost ($/h)	103.0597	100.7301
Total Cost ($/h)	782.5129	782.1910
Emission (t/h)	1.76231	1.76227
Power losses (MW)	5.7911	5.7823
V.D. (p.u.)	0.47399	0.46413

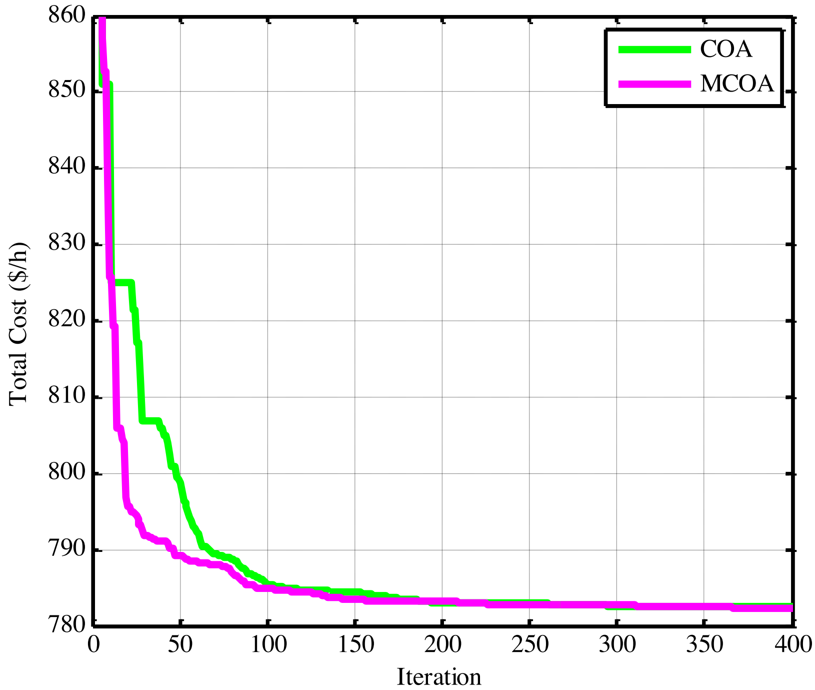

Figure 8: Convergence for case 7.

4.7.2 Case 8: Minimizing generating costs while accounting for the cost of carbon and the variable output of renewable sources

The threat of climate change has led some nations to raise their demands that the whole energy sector cut carbon emissions. *Ctax*, or carbon taxes, are charged on emissions of greenhouse gases.

This tax is intended to encourage financial investments in renewable energy sources like wind and solar power. The following is a breakdown, in USD per hour, of the cost of publishing (Biswas et al., 2018):

$$\text{Emission cost: } C_E = C_{tax}E \tag{50}$$

$$J_8 = J_7 + C_{tax}E \tag{51}$$

As a way of reducing the total costs associated with the generation of electrical power, the concluding case study of this article suggests imposing a financial penalty in the form of a carbon tax on the emissions of greenhouse gases by traditional thermal energy producers. The anticipated total cost of Equation (51) is what needs to be maintained at the lowest feasible level. It is anticipated that the rate of the carbon tax will be twenty dollars per ton.

Table 9 presents the results of a simulation conducted using these two methods to determine the ideal load distribution. The result produced by the proposed adjusted version of the algorithm is superior to that produced by the original method. More specifically, the pace of development of energy production programs based on renewable energy production will be decided by the volume of emissions and the degree of pricing and taxes on carbon. The convergent behavior of the two algorithms is shown in Figure 9 for case 8 of the research.

Table 9: The optimal variables value for case 8.

Variables	COA	MCOA
PG1 (MW)	123.98540	123.23593
PG2 (MW)	34.3509	32.2800
Pws1 (MW)	46.6899	45.6210
PG3 (MW)	10.0000	10.0000
Pws2 (MW)	39.2993	38.4229
Pss (MW)	34.3579	39.1160
VG1 (p.u.)	1.0704	1.0704
VG2 (p.u.)	1.0569	1.0569
VG5 (p.u.)	1.0359	1.0357
VG8 (p.u.)	1.1000	1.0403
VG11 (p.u.)	1.0983	1.0998
VG13 (p.u.)	1.0498	1.0566
QG1 (MVAR)	-2.97776	-2.74168
QG2 (MVAR)	11.05753	12.23749
Qws1 (MVAR)	22.23269	22.97597
QG3(MVAR)	40.00000	35.18169
Qws2 (MVAR)	30.00000	30.00000
Qss (MVAR)	15.37773	18.01536
Fuelvlvcost ($/h)	435.0921	426.2147
Wind gen cost ($/h)	264.8905	257.9513
Solar gen cost ($/h)	93.4094	108.8521
Total Cost ($/h)	793.3920	793.0180
Emission (t/h)	0.91514	0.87681
J8	811.6948	810.5542
Power losses (MW)	5.2833	5.2758
V.D. (p.u.)	0.45900	0.47042
Carbon tax ($/h)	18.3028	17.5362

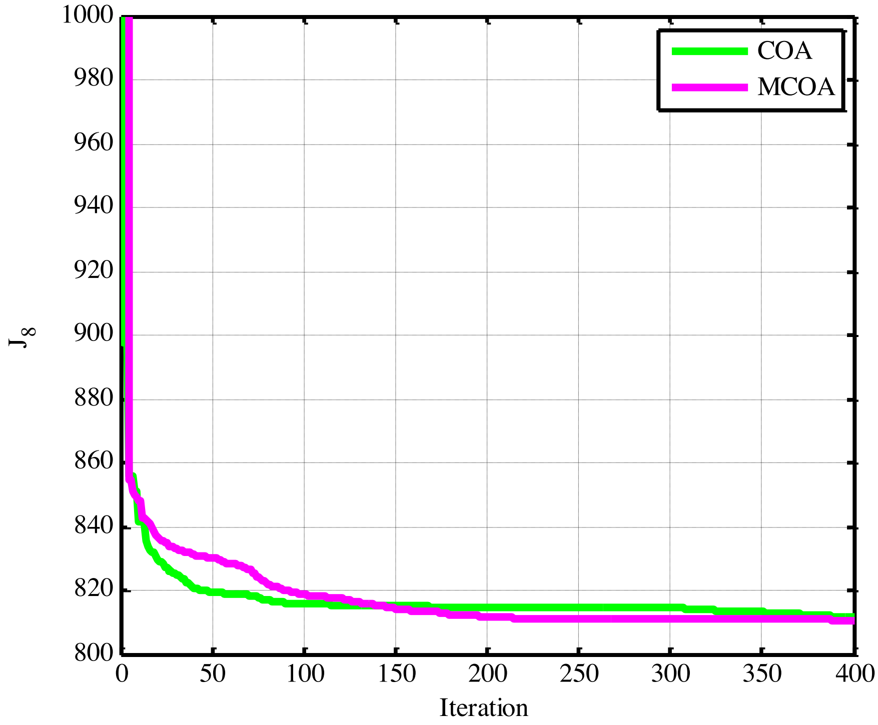

Figure 9: Convergence for case 8.

4.8 Discussions on the IEEE 30-bus network

In this section, we comprehensively compare between the suggested MCOA and the basic COA, and also, three modern powerful recent algorithms, arithmetic optimization algorithm (AOA) (Abualigah et al., 2021), weighted mean of vectors (INFO) (Ahmadianfar et al., 2022) and wild geese algorithm (WGA) (Ghasemi et al., 2021), over all of the scenarios covered in this article on the IEEE 30-bus network. Best, average, and worst results from 30 runs, as well as standard deviation and average running time, are shown in Table 10. An in-depth examination of this table demonstrates that the suggested MCOA method has triumphed over the original COA algorithm and three modern powerful recent algorithms, AOA, INFO and WGA in every situation tested and that it has done so without increasing the time it takes to execute the original algorithm or the complexity of the computations it conducts.

It is, therefore, evident that the suggested MCOA performs statistically differently from its competitors. According to these quantitative and qualitative findings, the proposed MCOA can produce challenging and competitive results at faster convergence speeds. Adopting a revolutionary hybrid optimization approach for the MCOA algorithm is proposed. This enhances its global search capability while balancing exploration and exploitation to achieve high-quality solutions. The algorithm can achieve better search efficiency by leveraging this approach and avoiding local optima. As part of the evaluation of the performance of the MCOA algorithm, it has been compared with the AOA, the INFO, the WGA, and the basic COA algorithms. As a result of the results, the suggested MCOA is superior and effective. The proposed algorithm has the advantage of fast convergence to global optima, making it suitable for solving complex real-world power system problems. We expect that as time progresses, the OPF problem will include emergency events, large-scale testing systems, and the penetration of electric vehicles.

Table 10: Statistical results of MCOA and COA.

Method	Min	Time (s)	Max	Mean	Std.
			Case 1		
AOA	802.6318	28.7	804.9570	803.7042	1.78
INFO	801.8834	30.4	804.3152	802.8556	2.93
WGA	800.9701	21.9	801.6926	801.2999	0.842
COA	801.7449	22.4	802.8623	802.0724	2.81
MCOA	800.4791	22.4	800.7816	800.5629	0.283
Method	Min	Time (s)	Max	Mean	Std.
			Case 2		
AOA	649.2593	26.9	651.5815	650.3662	2.46
INFO	647.7004	23.0	650.0457	648.9654	1.43
WGA	646.9731	21.1	647.3950	647.8821	0.749
COA	649.8857	22.5	651.1421	650.2790	1.94
MCOA	646.4890	22.5	646.9002	646.6874	0.375
Method	Min	Time (s)	Max	Mean	Std.
			Case 3		
AOA	833.7423	22.9	834.6465	835.9325	2.34
INFO	832.8083	29.7	834.3280	833.4100	1.12
WGA	832.4601	25.1	833.1994	832.7543	0.554
COA	832.8498	22.5	833.9849	833.3615	1.75
MCOA	832.2134	22.4	832.7816	832.5022	0.341
Method	Min	Time (s)	Max	Mean	Std.
			Case 4		
AOA	1041.5309	26.0	1042.8252	1042.0067	1.20
INFO	1040.9591	30.2	1042.3516	1041.8404	1.74
WGA	1040.3394	20.9	1040.9139	1040.6612	0.916
COA	1040.6773	22.4	1042.4279	1041.6434	1.96
MCOA	1040.0674	22.5	1040.6715	1040.3200	0.507
Method	Min	Time (s)	Max	Mean	Std.
			Case 5		

AOA	815.5255	28.1	817.6217	816.8410	1.01
INFO	814.3942	33.4	816.5601	815.5889	1.26
WGA	813.5269	23.8	814.2247	813.7112	0.604
COA	814.7277	22.5	816.2242	815.5209	1.25
MCOA	813.1276	22.5	813.7012	813.3723	0.429
Method	Min	Time (s)	Max	Mean	Std.
			Case 6		
AOA	968.4278	25.5	971.2885	970.2347	2.61
INFO	965.0305	29.0	970.4143	968.1889	2.43
WGA	964.8344	23.6	965.4578	965.6549	0.738
COA	968.0184	22.5	968.1634	967.0625	1.68
MCOA	964.2521	22.5	965.0307	964.5846	0.814
Method	Min	Time (s)	Max	Mean	Std.
			Case 7		
AOA	783.5939	27.6	785.2641	784.9991	0.977
INFO	782.4830	29.7	784.9170	783.3454	0.868
WGA	782.2985	25.4	782.9775	782.7531	0.852
COA	782.5129	26.4	783.9485	783.2901	1.34
MCOA	782.1910	26.4	782.7316	782.4721	0.663
Method	Min	Time (s)	Max	Mean	Std.
			Case 8		
AOA	812.7563	30.1	815.1569	814.3313	3.92
INFO	811.6345	32.3	814.2818	812.8100	2.84
WGA	810.6845	27.3	811.4569	811.1184	0.923
COA	811.6948	26.5	813.5013	812.1716	2.04
MCOA	810.5542	26.6	811.1652	810.8203	0.698

5. OPF in the IEEE 118-Bus large-scale test System

In this part, the IEEE 118-bus test system (Meng et al., 2021) is used to evaluate the efficiency of the proposed MCOA in solving a larger power system. This test system has 54 generators, 186 branches, 9 transformers, 2 reactors, and 12 capacitors. It has 129 control variables considered for 54 generator active powers and bus voltages, 9 transformer tap settings, and 12 shunt capacitor reactive power injections. All buses have voltage limitations between 0.94 and 1.06 p.u. Within the range of 0.90–1.10 p.u., the transformer tap settings are evaluated. Shunt capacitors have available reactive powers ranging from 0 to 30 MVAR (Duman, Rivera, et al., 2020).

5.1. Case 1: OPF problem with quadratic cost function for traditional generators without the solar and wind energy sources

In Tables 11 and 12, the result is compared to the results of other algorithms under investigation and some other techniques reported in the literature, including CS-GWO (Meng et al., 2021); MSA (Mohamed et al., 2017), FPA (Mohamed et al., 2017), MFO (Mohamed et al., 2017), PSOGSA (Mohamed et al., 2017), IABC (Bai et al., 2017), MCSA (Shaheen et al., 2021), MRao-2 and Rao algorithms (Hassan et al., 2021), SSO (Hassan et al., 2021), ICBO (Bouchekara et al., 2016), GWO (El-Fergany & Hasanien, 2015), and EWOA (Nadimi-Shahraki et al., 2021). According to this table, the MCOA outperforms various optimization techniques used to solve the large-scale OPF. According to the obtained simulation data, the minimum cost obtained from MCOA is 129517.37 $/h, which is less comparing to result of other algorithms. Also, Figure 10 depicts, after that, the convergence characteristic of the studied algorithms used in this case.

Table 11: Optimal decision variables settings for case 1.

Actual power output of generators									
PG1~ PG9	24.195	0.028	0.012	0.030	403.000	85.600	20.000	11.000	20.200
PG10~ PG18	0.015	195.982	281.021	10.918	7.149	15.998	0.183	5.000	48.300
PG19~ PG27	41.898	19.000	194.017	49.210	31.000	32.522	149.991	148.403	0.000
PG28~ PG36	354.500	350.903	458.220	0.000	0.000	0.000	15.822	19.620	0.000
PG3~ PG45	432.000	0.000	3.601	506.989	0.000	0.000	0.000	0.000	233.375
PG46~ PG54	37.885	0.220	3.998	29.041	6.000	35.000	36.500	0.011	0.000
Voltage magnitude of generators									
VG1~ VG9	1.020	1.038	1.040	1.075	1.100	1.029	1.036	1.042	1.028
VG10~ VG18	1.065	1.093	1.100	1.052	1.048	1.048	1.048	1.032	1.025
VG19~ VG27	1.021	1.049	1.060	1.031	1.027	1.029	1.049	1.068	1.055
VG28~ VG36	1.071	1.071	1.079	1.061	1.061	1.048	1.048	1.030	1.058
VG3~ VG45	1.069	1.080	1.078	1.092	1.068	1.075	1.076	1.600	1.061
VG46~ VG54	1.050	1.041	1.030	1.028	1.029	1.042	1.020	1.050	1.060
Transformers' tap									
T1~ T9	1.047	1.047	0.965	0.963	1.000	1.008	0.982	0.980	0.971
VAR compensating units									
QC1~QC9	30.000	0.000	0.000	2.000	20.000	8.000	8.000	28.235	28.748

QC10~QC14	29.9984	9.006	29.996	1.000	11.010	Cost ($/h)	129517.37	PLoss	76. 360

Table 12: Optimal results for case 1.

Optimizer	Min	Mean	Max	Std.	Time (s)
MCOA	129537.37	129549.25	129555.14	6.37	726
COA	138685.15	142950.74	144007.34	699.4	730
WGA	129540.44	129552.81	129558.95	8.93	703
AOA	139569.56	143175.14	145509.84	801.2	1134
INFO	138672.82	142884.29	143578.68	445.7	1378
CS-GWO (Meng et al., 2021)	129544.0	129558.9	129568.8	10.7	4252.5
PSOGSA (Mohamed et al., 2017)	129733.6	-	-	-	-
FPA (Mohamed et al., 2017)	129688.7	-	-	-	-
MFO (Mohamed et al., 2017)	129708.1	-	-	-	-
Rao-1 (Hassan et al., 2021)	131817.9	-	-	-	808.0
Rao-3 (Hassan et al., 2021)	131793.1	-	-	-	806.7
Rao-2 (Hassan et al., 2021)	131490.7	-	-	-	804.6
MRao-2 (Hassan et al., 2021)	131457.8	-	-	-	1160.3
EWOA (Nadimi-Shahraki et al., 2021)	140175.8	-	-	-	-
MCSA (Shaheen et al., 2021)	129873.6	-	-	-	-
ICBO (Bouchekara et al., 2016)	135121.6	-	-	-	-
MSA (Mohamed et al., 2017)	129640.7	-	-	-	-
SSO (Hassan et al., 2021)	132080.4	-	-	-	-
GWO (El-Fergany & Hasanien, 2015)	139948.1	142989.3	145484.6	797.8	1766.2
IABC (Bai et al., 2017)	129862.0	129895.0	-	40.8	4157.8

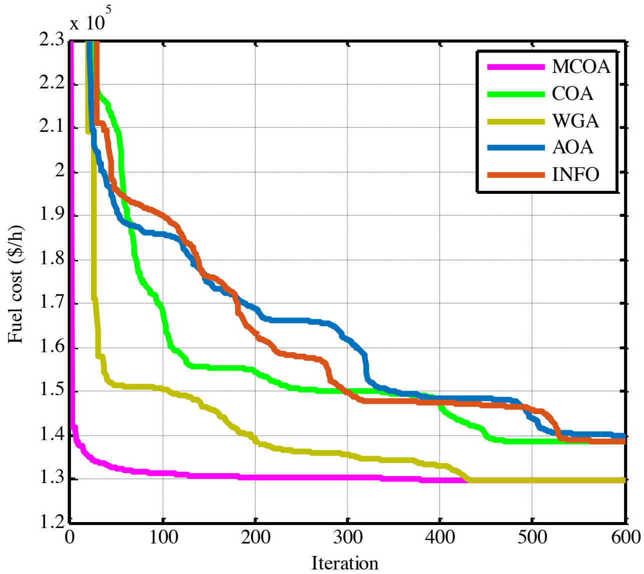

Figure 10: Convergence for case 1.

5.2. Case 2: OPF problem with quadratic cost function for traditional generators including the solar and wind energy sources.

Similar to the previous case system, wind energy sources are located in buses 18, 32, 36, 55, 104, and 110. Also, solar energy generation units are in nodes 6, 15 and 34. The best solution for this case is obtained by the proposed MCOA algorithm, as shown in Table 13. In addition, Table 14 represents a comparative study between the results of the algorithms studied in this article and the solutions obtained in the reference (Duman, Rivera, et al., 2020). From these results, the MCOA is a very powerful algorithm for optimizing and distributing optimization in large and real power systems. The characteristic of the convergence of the algorithms studied in this case is shown in Figure 11, demonstrating the good convergence performance of the proposed optimization algorithm.

In the case of the 118-bus system, OPF's superiority over MCOA is demonstrated as the system dimensions increase.

Table 13: Optimal decision variables settings for case 2.

Actual power output of generators									
PG1~ PG9	33.000	30.500	79.910 0	30.102	169.52 6	59.401	100.000	150.00 00	30.095
PG10~ PG18	30.505	96.011	144.98 2	30.000	32.103	120.00 0	149.655	120.00 0	30.082
PG19~ PG27	30.000 0	35.696	121.49 8	45.000	150.00 0	34.167	102.935	102.29 9	30.0
PG28~ PG36	202.17 7	205.48 9	273.78 0	30.200	30.200	30.200	30.000	30.100	30.100
PG3~ PG45	262.00 0	30.0	31.189	292.27 5	30.081	30.000	30.000	30.393	112.70 1

PG46~ PG54	42.000	145.00 0	30.000	30.009	120.00 0	401.00 0	30.001	30.050	30.001
Voltage magnitude of generators									
VG1~ VG9	0.9498	0.980	0.970	0.983	0.998	0.971	0.959	0.959	0.961
VG10~ VG18	0.974	0.974	0.983	0.974	0.958	0.972	0.961	0.953	0.946
VG19~ VG27	0.949	0.981	0.981	0.951	0.951	0.951	0.963	0.963	0.963
VG28~ VG36	0.970	1.025	1.025	0.975	0.987	0.987	0.955	0.955	0.979
VG3~ VG45	1.01	0.949	0.958	0.968	0.953	0.971	0.972	0.995	0.982
VG46~ VG54	0.980	0.948	0.960	0.9560	0.961	0.947	0.961	0.961	0.970
Transformers' tap									
T1~ T9	0.962	1.033	1.000	1.000	0.995	0.995	0.987	0.9890	0.941
VAR compensating units									
QC1~QC9	12.714	11.290 3	0.250	4.171	18.000	0.010	11.000	13.886	11.002
QC10~QC 14	6.557	13.001	23.357	1.106	5.999	Cost ($/h)	103395. 78	PLoss	55.119

Table 14: Optimal results for case 2.

Optimizer	Min	Mean	Max	Std.	Time (s)
MCOA	103395.78	103406.94	103415.67	10.42	781
COA	107008.21	109639.71	112617.55	818.2	759
WGA	103405.36	103412.05	103419.40	25.94	810
AOA	116994.05	120201.73	124011.65	1095.3	1240
INFO	106849.00	109114.19	113867.14	504.6	1405
DS (Duman, Rivera, et al., 2020)	110992.4249	112680.2902	114787.7786	953.6529	-
BSA (Duman, Rivera, et al., 2020)	117149.9833	120443.2982	123385.1256	1638.0949	-

MSA (Duman, Rivera, et al., 2020)	107695.0619	111205.0554	116303.6361	1857.2167	-
DEEPSO (Duman, Rivera, et al., 2020)	103407.6296	103889.1446	104507.4884	292.8782	-

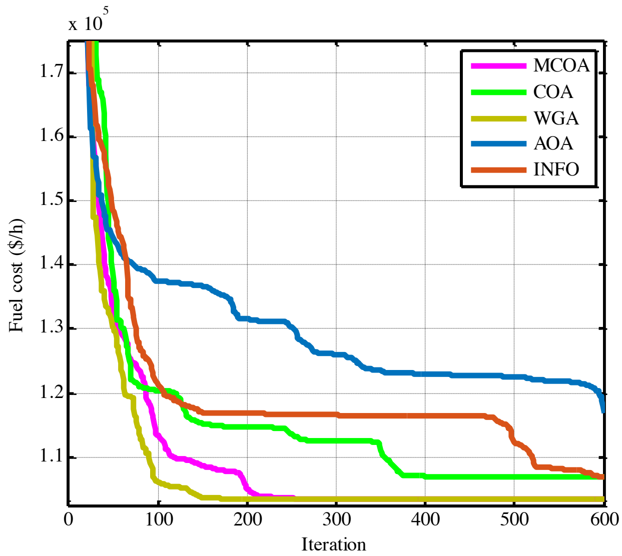

Figure 11: Convergence for case 2.

6 . Conclusion

The OPF problem, among various goals, is quickly becoming one of the most in-demand optimization problems in today's modern power networks. This article investigates multiple multiobjective OPF challenges, including renewable energy. A wide range of possible scenarios are considered considering power systems' complexities and constraints. These concerns include power loss, fuel expense, environmental effects, and voltage deviation values. In addition, a modified version of the Cuckoo optimization algorithm (COA) (MCOA) is built. A variety of algorithms have been developed for optimal multiobjective OPF under a variety of circumstances. Studies have demonstrated the efficiency and reliability of the MCOA algorithm in solving OPF problems in the presence of renewable DG resources.

References

Abaci, K., & Yamacli, V. (2016). Differential search algorithm for solving multi-objective optimal power flow problem. *International Journal of Electrical Power & Energy Systems*, *79*, 1–10. https://doi.org/10.1016/j.ijepes.2015.12.021

Abido, M. A. (2002). Optimal Power Flow Using Tabu Search Algorithm. *Electric Power Components and Systems*, *30*(5), 469–483. https://doi.org/10.1080/15325000252888425

Abualigah, L., Diabat, A., Mirjalili, S., Abd Elaziz, M., & Gandomi, A. H. (2021). The arithmetic optimization algorithm. *Computer Methods in Applied Mechanics and Engineering*, *376*, 113609.

Ahmad, M., Javaid, N., Niaz, I. A., Almogren, A., & Radwan, A. (2021). A Bio-Inspired Heuristic Algorithm for Solving Optimal Power Flow Problem in Hybrid Power System. *IEEE Access*, *9*, 159809–159826.

Ahmadianfar, I., Heidari, A. A., Noshadian, S., Chen, H., & Gandomi, A. H. (2022). INFO: An efficient optimization algorithm based on weighted mean of vectors. *Expert Systems with Applications*, *195*, 116516. https://doi.org/10.1016/j.eswa.2022.116516

Alsac, O., & Stott, B. (1974). Optimal load flow with steady-state security. *IEEE Transactions on Power Apparatus and Systems*, *3*, 745–751.

Attia, A.-F., El Sehiemy, R. A., & Hasanien, H. M. (2018). Optimal power flow solution in power systems using a novel Sine-Cosine algorithm. *International Journal of Electrical Power & Energy Systems*, *99*, 331–343. https://doi.org/10.1016/j.ijepes.2018.01.024

Bai, W., Eke, I., & Lee, K. Y. (2017). An improved artificial bee colony optimization algorithm based on orthogonal learning for optimal power flow problem. *Control Engineering Practice*, *61*, 163–172.

Bentouati, B., Khelifi, A., Shaheen, A. M., & El-Sehiemy, R. A. (2020). An enhanced moth-swarm algorithm for efficient energy management based multi dimensions OPF problem. *Journal of Ambient Intelligence and Humanized Computing*, 1–21. https://doi.org/10.1007/s12652-020-02692-7

Biswas, P. P., Suganthan, P. N., Mallipeddi, R., & Amaratunga, G. A. J. (2018). Optimal power flow solutions using differential evolution algorithm integrated with effective constraint handling techniques. *Engineering Applications of Artificial Intelligence*, *68*, 81–100. https://doi.org/10.1016/j.engappai.2017.10.019

Bouchekara, H. R. E. H., Chaib, A. E., Abido, M. A., & El-Sehiemy, R. A. (2016). Optimal power flow using an Improved Colliding Bodies Optimization algorithm. *Applied Soft Computing*, *42*, 119–131. https://doi.org/10.1016/j.asoc.2016.01.041

Chen, G., Qian, J., Zhang, Z., & Sun, Z. (2019). Multi-objective optimal power flow based on hybrid firefly-bat algorithm and constraints-prior object-fuzzy sorting strategy. *IEEE Access*, *7*, 139726–139745.

Dalali, M., & Kazemi Karegar, H. (2016). Optimal PMU placement for full observability of the power network with maximum redundancy using modified binary cuckoo optimisation algorithm. *IET Generation, Transmission \& Distribution*, *10*(11), 2817–2824.

Daryani, N., Hagh, M. T., & Teimourzadeh, S. (2016). Adaptive group search optimization algorithm for multi-objective optimal power flow problem. *Applied Soft Computing*, *38*, 1012–1024. https://doi.org/10.1016/j.asoc.2015.10.057

Dasgupta, K., Roy, P. K., & Mukherjee, V. (2020). Power flow based hydro-thermal-wind scheduling of hybrid power system using sine cosine algorithm. *Electric Power Systems Research*, *178*, 106018.

Dehghanpour, E., Karegar, H. K., Kheirollahi, R., & Soleymani, T. (2016). Optimal coordination of directional overcurrent relays in microgrids by using cuckoo-linear optimization algorithm and fault current limiter. *IEEE Transactions on Smart Grid*, *9*(2), 1365–1375.

Duman, S., Akbel, M., & Kahraman, H. T. (2021). Development of the multi-objective adaptive guided differential evolution and optimization of the MO-ACOPF for wind/PV/tidal energy sources. *Applied Soft Computing*, *112*, 107814.

Duman, S., Li, J., Wu, L., & Guvenc, U. (2020). Optimal power flow with stochastic wind power and FACTS devices: A modified hybrid PSOGSA with chaotic maps approach. *Neural Computing and Applications*, *32*(12), 8463–8492. https://doi.org/10.1007/s00521-019-04338-y

Duman, S., Rivera, S., Li, J., & Wu, L. (2020). Optimal power flow of power systems with controllable wind-photovoltaic energy systems via differential evolutionary particle swarm optimization. *International Transactions on Electrical Energy Systems*, *30*(4), e12270. https://doi.org/10.1002/2050-7038.12270

El Sehiemy, R. A., Selim, F., Bentouati, B., & Abido, M. A. (2020). A novel multi-objective hybrid particle swarm and salp optimization algorithm for technical-economical-environmental operation in power systems. *Energy*, *193*, 116817.

Elattar, E. E. (2019). Optimal power flow of a power system incorporating stochastic wind power based on modified moth swarm algorithm. *IEEE Access*, *7*, 89581–89593.

Elattar, E. E., & ElSayed, S. K. (2019). Modified JAYA algorithm for optimal power flow incorporating renewable energy sources considering the cost, emission, power loss and voltage profile improvement. *Energy*, *178*, 598–609. https://doi.org/10.1016/j.energy.2019.04.159

El-Fergany, A. A., & Hasanien, H. M. (2015). Single and Multi-objective Optimal Power Flow Using Grey Wolf Optimizer and Differential Evolution Algorithms. *Electric Power Components and Systems*, *43*(13), 1548–1559. https://doi.org/10.1080/15325008.2015.1041625

El-Sehiemy, R. A. (2022). A novel single/multi-objective frameworks for techno-economic operation in power systems using tunicate swarm optimization technique. *Journal of Ambient Intelligence and Humanized Computing*, 1–19.

Ghasemi, M., Ghavidel, S., Akbari, E., & Vahed, A. A. (2014). Solving non-linear, non-smooth and non-convex optimal power flow problems using chaotic invasive weed optimization algorithms based on chaos. *Energy*, *73*, 340–353. https://doi.org/10.1016/j.energy.2014.06.026

Ghasemi, M., Ghavidel, S., Ghanbarian, M. M., Gharibzadeh, M., & Azizi Vahed, A. (2014). Multi-objective optimal power flow considering the cost, emission, voltage deviation and power losses using multi-objective modified imperialist competitive algorithm. *Energy*, *78*, 276–289. https://doi.org/10.1016/j.energy.2014.10.007

Ghasemi, M., Ghavidel, S., Ghanbarian, M. M., & Gitizadeh, M. (2015). Multi-objective optimal electric power planning in the power system using Gaussian bare-bones imperialist competitive algorithm. *Information Sciences*, *294*. https://doi.org/10.1016/j.ins.2014.09.051

Ghasemi, M., Ghavidel, S., Gitizadeh, M., & Akbari, E. (2015). An improved teaching–learning-based optimization algorithm using Lévy mutation strategy for non-smooth optimal power flow. *International Journal of Electrical Power & Energy Systems*, *65*, 375–384. https://doi.org/10.1016/j.ijepes.2014.10.027

Ghasemi, M., Ghavidel, S., Rahmani, S., Roosta, A., & Falah, H. (2014). A novel hybrid algorithm of imperialist competitive algorithm and teaching learning algorithm for optimal power flow problem with non-smooth cost functions. *Engineering Applications of Artificial Intelligence*, *29*, 54–69. https://doi.org/10.1016/j.engappai.2013.11.003

Ghasemi, M., Rahimnejad, A., Hemmati, R., Akbari, E., & Gadsden, S. A. (2021). Wild Geese Algorithm: A novel algorithm for large scale optimization based on the natural life and death of wild geese. *Array*, *11*, 100074.

Ghoneim, S. S. M., Kotb, M. F., Hasanien, H. M., Alharthi, M. M., & El-Fergany, A. A. (2021). Cost

Minimizations and Performance Enhancements of Power Systems Using Spherical Prune Differential Evolution Algorithm Including Modal Analysis. *Sustainability*, *13*(14), 8113.

Gupta, S., Kumar, N., Srivastava, L., Malik, H., Pliego Marugán, A., & Garc\'\ia Márquez, F. P. (2021). A Hybrid Jaya—Powell's Pattern Search Algorithm for Multi-Objective Optimal Power Flow Incorporating Distributed Generation. *Energies*, *14*(10), 2831.

Guvenc, U., Bakir, H., Duman, S., & Ozkaya, B. (2020). Optimal Power Flow Using Manta Ray Foraging Optimization. *The International Conference on Artificial Intelligence and Applied Mathematics in Engineering*, 136–149.

Hassan, M. H., Elsayed, S. K., Kamel, S., Rahmann, C., & Taha, I. B. M. (n.d.). Developing chaotic Bonobo optimizer for optimal power flow analysis considering stochastic renewable energy resources. *International Journal of Energy Research*.

Hassan, M. H., Kamel, S., Selim, A., Khurshaid, T., & Domínguez-García, J. L. (2021). A modified Rao-2 algorithm for optimal power flow incorporating renewable energy sources. *Mathematics*, *9*(13), 1532.

Hazra, J., & Sinha, A. K. (2011). A multi-objective optimal power flow using particle swarm optimization. *European Transactions on Electrical Power*, *21*(1), 1028–1045. https://doi.org/10.1002/etep.494

Herbadji, O., Slimani, L., & Bouktir, T. (2019). Optimal power flow with four conflicting objective functions using multiobjective ant lion algorithm: A case study of the algerian electrical network. *Iranian Journal of Electrical and Electronic Engineering*, *15*(1), 94–113. https://doi.org/10.22068/IJEEE.15.1.94

Islam, M. Z., Wahab, N. I. A., Veerasamy, V., Hizam, H., Mailah, N. F., Guerrero, J. M., & Mohd Nasir, M. N. (2020). A Harris Hawks optimization based single- and multi-objective optimal power flow considering environmental emission. *Sustainability*, *12*(13), 5248.

Jebaraj, L., & Sakthivel, S. (2022). A new swarm intelligence optimization approach to solve power flow optimization problem incorporating conflicting and fuel cost based objective functions. *E-Prime-Advances in Electrical Engineering, Electronics and Energy*, *2*, 100031.

Kahraman, H. T., Akbel, M., & Duman, S. (2022). Optimization of optimal power flow problem using multi-objective manta ray foraging optimizer. *Applied Soft Computing*, *116*, 108334.

Kamel, S., Ebeed, M., & Jurado, F. (2021). An improved version of salp swarm algorithm for solving optimal power flow problem. *Soft Computing*, *25*(5), 4027–4052.

Khamees, A. K., Abdelaziz, A. Y., Eskaros, M. R., El-Shahat, A., & Attia, M. A. (2021). Optimal Power Flow Solution of Wind-Integrated Power System Using Novel Metaheuristic Method. *Energies*, *14*(19), 6117.

Khan, I. U., Javaid, N., Gamage, K. A. A., Taylor, C. J., Baig, S., & Ma, X. (2020). Heuristic algorithm based optimal power flow model incorporating stochastic renewable energy sources. *IEEE Access*, *8*, 148622–148643.

Khorsandi, A., Hosseinian, S. H., & Ghazanfari, A. (2013). Modified artificial bee colony algorithm based on fuzzy multi-objective technique for optimal power flow problem. *Electric Power Systems Research*, *95*, 206–213. https://doi.org/10.1016/j.epsr.2012.09.002

Kumari, B. A., & Vaisakh, K. (2022). Integration of solar and flexible resources into expected security cost with dynamic optimal power flow problem using a Novel DE algorithm. *Renewable Energy Focus*.

Kyomugisha, R., Muriithi, C. M., & Nyakoe, G. N. (2022). Performance of Various Voltage Stability Indices in a Stochastic Multiobjective Optimal Power Flow Using Mayfly Algorithm. *Journal of Electrical and Computer Engineering*, *2022*.

Li, S., Gong, W., Wang, L., Yan, X., & Hu, C. (2020). Optimal power flow by means of improved adaptive differential evolution. *Energy*, *198*, 117314. https://doi.org/10.1016/j.energy.2020.117314

Ma, R., Li, X., Luo, Y., Wu, X., & Jiang, F. (2019). Multi-objective dynamic optimal power flow of wind integrated power systems considering demand response. *CSEE Journal of Power and Energy Systems*, *5*(4), 466–473.

Maheshwari, A., Sood, Y. R., Jaiswal, S., Sharma, S., & Kaur, J. (2021). Ant Lion Optimization Based OPF Solution Incorporating Wind Turbines and Carbon Emissions. *2021 Innovations in Power and Advanced Computing Technologies (i-PACT)*, 1–6.

Meng, A., Zeng, C., Wang, P., Chen, D., Zhou, T., Zheng, X., & Yin, H. (2021). A high-performance crisscross search based grey wolf optimizer for solving optimal power flow problem. *Energy*, *225*, 120211.

Mohamed, A.-A. A., Mohamed, Y. S., El-Gaafary, A. A. M., & Hemeida, A. M. (2017). Optimal power flow using moth swarm algorithm. *Electric Power Systems Research*, *142*, 190–206. https://doi.org/10.1016/j.epsr.2016.09.025

Mohapatra, P., Chakravarty, S., & Dash, P. K. (2015). An improved cuckoo search based extreme learning machine for medical data classification. *Swarm and Evolutionary Computation*, *24*, 25–49.

Nadimi-Shahraki, M. H., Taghian, S., Mirjalili, S., Abualigah, L., Abd Elaziz, M., & Oliva, D. (2021). EWOA-OPF: Effective Whale Optimization Algorithm to Solve Optimal Power Flow Problem. *Electronics*, *10*(23), 2975.

Narimani, M. R., Azizipanah-Abarghooee, R., Zoghdar-Moghadam-Shahrekohne, B., & Gholami, K. (2013). A novel approach to multi-objective optimal power flow by a new hybrid optimization algorithm considering generator constraints and multi-fuel type. *Energy*, *49*, 119–136. https://doi.org/10.1016/j.energy.2012.09.031

Nguyen, T. T. (2019). A high performance social spider optimization algorithm for optimal power flow solution with single objective optimization. *Energy*, *171*, 218–240. https://doi.org/10.1016/j.energy.2019.01.021

Niknam, T., Narimani, M. R., Aghaei, J., Tabatabaei, S., & Nayeripour, M. (2011). Modified Honey Bee Mating Optimisation to solve dynamic optimal power flow considering generator constraints. *IET*

Generation, Transmission & Distribution, *5*(10), 989. https://doi.org/10.1049/iet-gtd.2011.0055

Niknam, T., Narimani, M. rasoul, Jabbari, M., & Malekpour, A. R. (2011). A modified shuffle frog leaping algorithm for multi-objective optimal power flow. *Energy*, *36*(11), 6420–6432. https://doi.org/10.1016/j.energy.2011.09.027

Ongsakul, W., & Tantimaporn, T. (2006). Optimal Power Flow by Improved Evolutionary Programming. *Electric Power Components and Systems*, *34*(1), 79–95. https://doi.org/10.1080/15325000691001458

Ouafa, H., Linda, S., & Tarek, B. (2017). Multi-objective optimal power flow considering the fuel cost, emission, voltage deviation and power losses using Multi-Objective Dragonfly algorithm. *Proceedings of the International Conference on Recent Advances in Electrical Systems, Tunusia*.

Panda, A., Tripathy, M., Barisal, A. K., & Prakash, T. (2017). A modified bacteria foraging based optimal power flow framework for Hydro-Thermal-Wind generation system in the presence of STATCOM. *Energy*, *124*, 720–740. https://doi.org/10.1016/j.energy.2017.02.090

Pulluri, H., Naresh, R., & Sharma, V. (2018). A solution network based on stud krill herd algorithm for optimal power flow problems. *Soft Computing*, *22*(1), 159–176. https://doi.org/10.1007/s00500-016-2319-3

Radosavljević, J., Klimenta, D., Jevtić, M., & Arsić, N. (2015). Optimal Power Flow Using a Hybrid Optimization Algorithm of Particle Swarm Optimization and Gravitational Search Algorithm. *Electric Power Components and Systems*, *43*(17), 1958–1970. https://doi.org/10.1080/15325008.2015.1061620

Rajabioun, R. (2011). Cuckoo optimization algorithm. *Applied Soft Computing*, *11*(8), 5508–5518.

Ramesh Kumar, A., & Premalatha, L. (2015). Optimal power flow for a deregulated power system using adaptive real coded biogeography-based optimization. *International Journal of Electrical Power & Energy Systems*, *73*, 393–399. https://doi.org/10.1016/j.ijepes.2015.05.011

Riaz, M., Hanif, A., Hussain, S. J., Memon, M. I., Ali, M. U., & Zafar, A. (2021). An optimization-based strategy for solving optimal power flow problems in a power system integrated with stochastic solar and wind power energy. *Applied Sciences*, *11*(15), 6883.

Roy, R., & Jadhav, H. T. (2015). Optimal power flow solution of power system incorporating stochastic wind power using Gbest guided artificial bee colony algorithm. *International Journal of Electrical Power & Energy Systems*, *64*, 562–578. https://doi.org/10.1016/j.ijepes.2014.07.010

Saha, A., Bhattacharya, A., Das, P., & Chakraborty, A. K. (2019). A novel approach towards uncertainty modeling in multiobjective optimal power flow with renewable integration. *International Transactions on Electrical Energy Systems*, *29*(12), e12136. https://doi.org/10.1002/2050-7038.12136

Sarda, J., Pandya, K., & Lee, K. Y. (2021). Hybrid cross entropy—Cuckoo search algorithm for solving optimal power flow with renewable generators and controllable loads. *Optimal Control Applications and Methods*.

Sarhan, S., El-Sehiemy, R., Abaza, A., & Gafar, M. (2022). Turbulent Flow of Water-Based Optimization for Solving Multi-Objective Technical and Economic Aspects of Optimal Power Flow Problems. *Mathematics*, *10*(12), 2106.

Sayah, S., & Zehar, K. (2008). Modified differential evolution algorithm for optimal power flow with non-smooth cost functions. *Energy Conversion and Management*, *49*(11), 3036–3042. https://doi.org/10.1016/j.enconman.2008.06.014

Shaheen, A. M., El-Sehiemy, R. A., Elattar, E. E., & Abd-Elrazek, A. S. (2021). A modified crow search optimizer for solving non-linear OPF problem with emissions. *IEEE Access*, *9*, 43107–43120.

Shi, L., Wang, C., Yao, L., Ni, Y., & Bazargan, M. (2011). Optimal power flow solution incorporating wind power. *IEEE Systems Journal*, *6*(2), 233–241.

Shilaja, C., & Ravi, K. (2017). Optimal power flow using hybrid DA-APSO algorithm in renewable energy resources. *Energy Procedia*, *117*, 1085–1092.

SOOD, Y. (2007). Evolutionary programming based optimal power flow and its validation for deregulated power system analysis. *International Journal of Electrical Power & Energy Systems*, *29*(1), 65–75. https://doi.org/10.1016/j.ijepes.2006.03.024

Ullah, Z., Wang, S., Radosavljević, J., & Lai, J. (2019). A solution to the optimal power flow problem considering WT and PV generation. *IEEE Access*, *7*, 46763–46772.

Venkateswara Rao, B., & Nagesh Kumar, G. V. (2015). Optimal power flow by BAT search algorithm for generation reallocation with unified power flow controller. *International Journal of Electrical Power & Energy Systems*, *68*, 81–88. https://doi.org/10.1016/j.ijepes.2014.12.057

Warid, W., Hizam, H., Mariun, N., & Abdul Wahab, N. I. (2018). A novel quasi-oppositional modified Jaya algorithm for multi-objective optimal power flow solution. *Applied Soft Computing*, *65*, 360–373. https://doi.org/10.1016/j.asoc.2018.01.039

Warid, W., Hizam, H., Mariun, N., & Abdul-Wahab, N. (2016). Optimal Power Flow Using the Jaya Algorithm. *Energies*, *9*(9), 678. https://doi.org/10.3390/en9090678

Xiao, L., Shao, W., Yu, M., Ma, J., & Jin, C. (2017). Research and application of a hybrid wavelet neural network model with the improved cuckoo search algorithm for electrical power system forecasting. *Applied Energy*, *198*, 203–222.

Yuan, X., Zhang, B., Wang, P., Liang, J., Yuan, Y., Huang, Y., & Lei, X. (2017). Multi-objective optimal power flow based on improved strength Pareto evolutionary algorithm. *Energy*, *122*, 70–82. https://doi.org/10.1016/j.energy.2017.01.071

Zeynal, H., Hui, L. X., Jiazhen, Y., Eidiani, M., & Azzopardi, B. (2014). Improving lagrangian relaxation unit commitment with cuckoo search algorithm. *2014 IEEE International Conference on Power and Energy (PECon)*, 77–82.

Zhang, J., Wang, S., Tang, Q., Zhou, Y., & Zeng, T. (2019). An improved NSGA-III integrating adaptive elimination strategy to solution of many-objective optimal power flow problems. *Energy*, *172*, 945–957.

Zimmerman, R. D., Murillo-Sanchez, C. E., & Thomas, R. J. (n.d.). Feb 2011. MATPOWER: Steady-State Operations, Planning, and Analysis Tools for Power Systems Research and Education, 26(1), 12–19.